Ion Conduction in Composite Polymer Electrolytes: Potential Electrolytes for Sodium-Ion Batteries
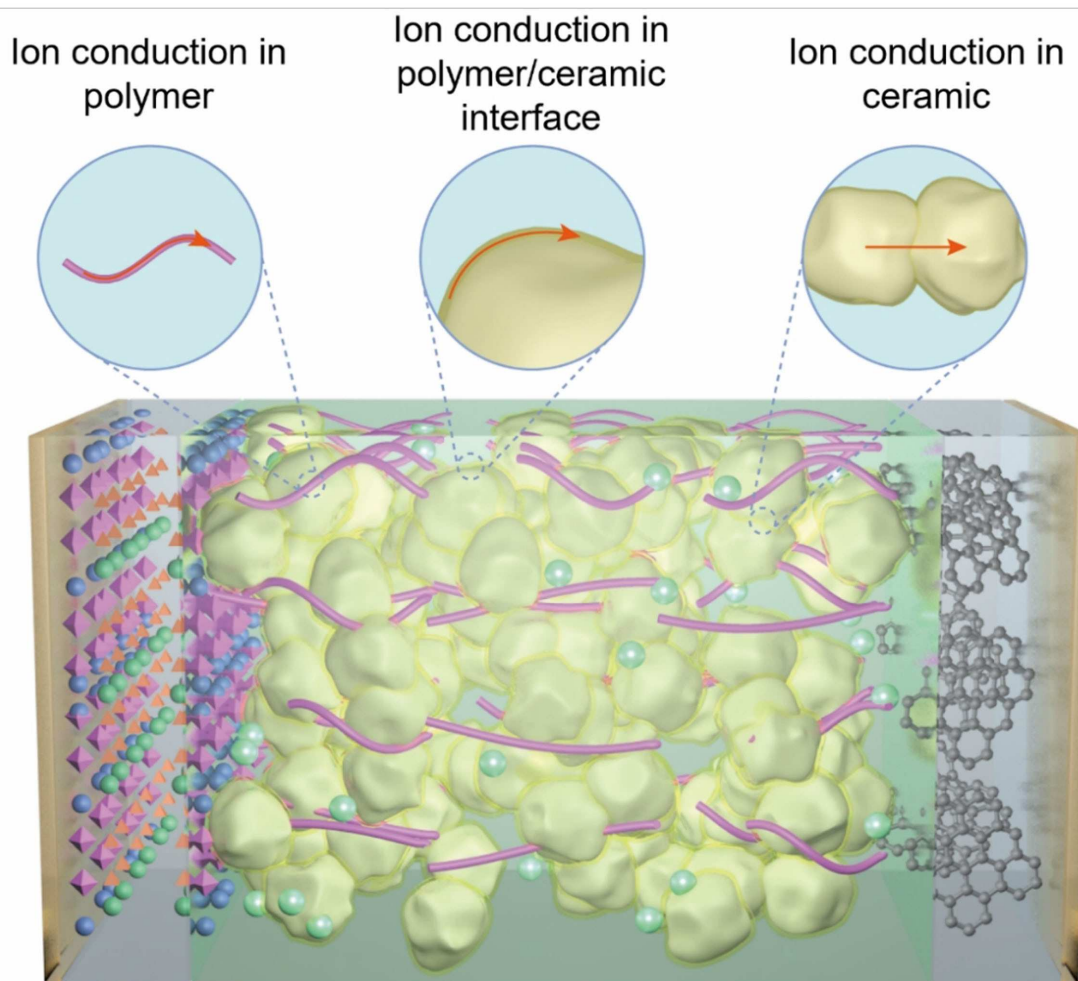
Xiaoyu Xu,[a, b] Yumei Wang,*[a] Qiang Yi,[a] Xinyu Wang,[a, b]
Ramon Alberto Paredes Camacho,[a] Hans Kungl,[c] Ruediger Eichel,[c] Li Lu,*[a, b] and
Huangwei Zhang*[a, b]

ChemSusChem

Review

doi.org/10.1002/cssc.202202152

Chemistry
Europe
European Chemical
Societies Publishing

Sodium-ion batteries (SIBs) are expected to become alternatives to lithium-ion batteries (LIBs) as next-generation rechargeable batteries, owing to abundant sodium sources and low cost. However, SIBs still use liquid organic electrolytes (LOEs), which are highly flammable and have the tendency to leak. Although inorganic solid electrolytes (ISEs) and solid polymer electrolytes (SPEs) have been investigated for many years, given their higher safety level, neither of them is likely to be commercialized because of the rigidity of ISEs and the low room-temperature ionic conductivity of SPEs. During the last decade, composite polymer electrolytes (CPEs), composed of ISEs and SPEs, exhibiting both relatively high ionic conductivity and flexibility, have gained much attention and are considered as promising electrolytes. However, the ionic conductivities of CPEs are still unsatisfactory for practical application. Hence, this Review focuses on the principle of sodium ion conductors and particularly on recent investigations and development of CPEs.

1. Introduction

Energy conversion and storage have become a hot research direction in the field of materials science because energy is an important basis for human survival and development.[1–3] However, with the continuous increasing demand for energy, energy systems based on fossil fuels not only support the social development, but also lay great hidden dangers for the sustainable development of the earth.[4,5] It is necessary to accelerate the transition to green and low-carbon energy for the purpose of reducing the dependence on fossil fuels.[6] Many alternative energy sources like wind and solar have been used for generating electricity,[7] which are clean and sustainable energy sources. However, solar and wind cannot offer a continuous and reliable power supply, which means they are intermittent, and require large-scale energy storage systems with low cost to keep balance between supply and demand.[8–10]

In the past three decades, lithium-ion batteries (LIBs) have been quickly developed on account of high specific energy densities and long cycle life.[11–13] Currently, with the best comprehensive performance, LIBs are widely being used and dominate the market of portable devices and electric vehicles.[14–16] Nevertheless, the lack of lithium sources and increasing prices force people to find affordable alternatives for LIBs. Sodium, as one of the most abundant sources in the world, comes from the same group with lithium in the periodic table.[17,18] They have similar chemical properties and the working principles of LIBs and Sodium-ion batteries (SIBs) are basically the same.[19,20] The energy density of SIBs is not comparable to LIBs due to the larger ionic radius[21] and they

cannot replace LIBs in the field of portable devices, but they can play a good role in the large-scale energy storage systems for low cost and environmental friendliness.[22]

Another most concerned problem is the safety issues of commercialized LIBs using liquid organic electrolytes (LOEs).[23] Many accidents have happened due to the leakage and flammability of LOEs.[24,25] To solve the safety risks, solid state electrolytes (SSEs) with improved chemical and electrochemical stability and absent leakage have drawn more and more attention.[26] SSEs can also realize the application of sodium metal as anode to enhance the energy densities of SIBs,[27] whereas LOEs cannot use sodium metal for the continuous side reactions.[28,29] Good SSEs should possess the following requisites,[30,31] including not only high ionic conductivity, transference number and stability but also good mechanical strength, ability to inhibit dendrites and interface contact with electrodes. Compared with LOEs, SSEs have many advantages but poorer ionic conductivities. Generally speaking, the ionic conductivities of LOEs can reach up to 10^{-2} S cm^{-1}[32] and much higher than that of SSEs.[33] The relatively highest ionic conductivity of SSEs can reach up to about 10^{-4} S cm^{-1}. For practical application, the ionic conductivity of existing SSEs is not high enough.

The classification of SSEs can be divided into three kinds, which are inorganic solid electrolytes (ISEs), solid polymer electrolytes (SPEs) and composite polymer electrolytes (CPEs).[34,35] ISEs are mainly ceramic crystals, they exhibit high ionic conductivity of about 10^{-3}–10^{-4} S cm^{-1} under room temperature and the transference number of sodium ion migration number is close to 1. However, ceramics are rigid and brittle, the contact between ISEs and electrode is a solid–solid contact and will lead to a high interface resistance.[36] SPEs generally show a low ionic conductivity of about 10^{-7} S cm^{-1} under room temperature,[37] but its excellent interfacial compatibility with electrodes resulting in a low interfacial resistance is beneficial to the practical application.[38,39] CPEs, who combine both the relatively high ionic conductivity of ISEs and flexibility of SPEs, gain much attention. Despite CPEs have the ability to realize the purpose of high energy density and high safety, the ion conduction mechanisms still have a dispute over which component plays the crucial role in the migration of alkali metal ions. To further improve the ionic conductivities of SSEs, ion conduction mechanism should be understood.

Quite a few review articles discussed about the CPEs for LIBs because LIBs have always been a hot research topic since its successful application in 1991.[40–44] Although SIBs are becoming

[a] X. Xu, Dr. Y. Wang, Q. Yi, X. Wang, Dr. R. A. Paredes Camacho, Prof. L. Lu, Prof. H. Zhang
National University of Singapore (Chongqing) Research Institute
401123 Chongqing (P. R. China)
E-mail: yumei.wang@nusricq.cn

[b] X. Xu, X. Wang, Prof. L. Lu, Prof. H. Zhang
Department of Mechanical Engineering, National University of Singapore
9 Engineering Drive 1, 117575 Singapore (Singapore)
E-mail: luli@nus.edu.sg
huangwei.zhang@nus.edu.sg

[c] Prof. H. Kungl, Prof. R. Eichel
Fundamental electrochemistry (IEK-9)
Institute of Energy and Climate Research
Forschungszentrum Jülich, 52425 Jülich (Germany)

ChemSusChem

Review
doi.org/10.1002/cssc.202202152

Chemistry Europe
European Chemical
Societies Publishing

more and more popular, the review articles focus on CPEs for SIBs are few.[45] As the most competitive candidates for next-generation electrolytes and rechargeable batteries, more efforts should be done to the further development of CPEs for SIBs. This review summarizes the principles of sodium ion conductors and ion conduction mechanisms in composite polymer electrolytes for sodium-ion batteries via recent investigations and developments of CPEs.

2. Ion Conduction in Polymers

Solid polymer electrolytes (SPEs) for SIBs are basically composed of polymer matrices and additive sodium salts. The ion conduction in solid polymers relies on the sodium ions migration between ion coordination sites. There are two possible kinds of sodium ion transport in host polymers, happening in amorphous and crystalline phases respectively. The first mechanism is the most commonly accepted conduction mechanism of sodium ions in SPEs, which depends on the motion of segmental chains of host polymers.[46] Figure 1a shows that the polymer segmental chains can move in amorphous regions above the glass transition temperature (T_g) to help complete the transport of sodium ions. Therefore, this kind of mechanism is closely related to T_g.[42,47,48] The other kind happens in the crystalline phases of polymers because majority of the polymers are not totally amorphous. The crystalline regions in semi-crystalline polymers do not have a segmental motion. Under the first mechanism, the crystalline region is
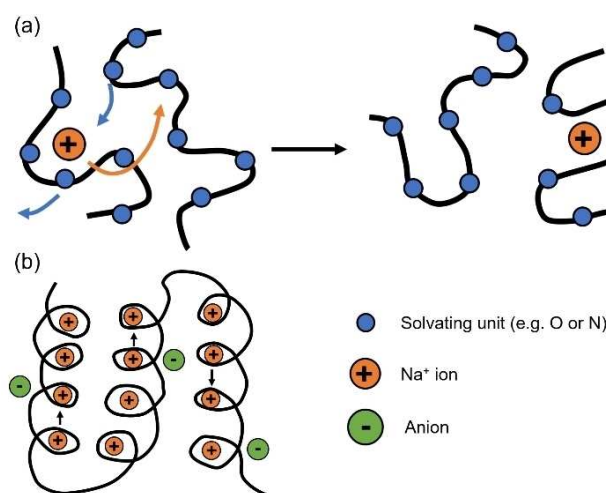

Figure 1. (a) Ion conduction mechanism in amorphous regions of polymer. Reproduced with permission.[46] Copyright 2021, Elsevier. (b) Ion conduction mechanism in crystalline regions of polymer. Reproduced with permission.[50] Copyright 1982, American Chemical Society.

supposed to impede the transport of sodium ions and the approach to increase the ionic conductivity is decreasing the crystallinity of host polymers.[49] However, it has been proved that the sodium ions can still transport in the crystalline regions of host polymers.[50–53] In this situation, sodium ions are supposed to reside in the helical tunnels (Figure 1b) formed by

Xiaoyu Xu received her bachelor's degree from Soochow University in 2020 and master degree from National University of Singapore in 2021. Currently, she is a Ph.D. student in Department of Mechanical Engineering at National University of Singapore. Her research interests include solid-state/quasi-solid-state electrolytes for rechargeable batteries.

Dr. Yumei Wang received her Ph.D. degree at National University of Singapore (NUS, Singapore) in 2018. Later, she works as a postdoctoral research fellow in NUS from 2018 to 2020. In 2021, she joins in National University of Singapore Chongqing Research Institute (NUSRI-CQ) and works as a research fellow. Her research interests include advanced materials for rechargeable batteries/solid-state batteries/quasi-solid batteries and ferroelectric/piezoelectric/dielectric ceramic films for microelectromechanical system (MEMS) transducers/sensors.

Dr. Li Lu is a Professor at the Department of Mechanical Engineering of National University of Singapore and the Deputy Director at NUS (Chongqing) Research Institute. He got his bachelor and master degree from Tsinghua University in 1977 and 1982. Later he obtained his Ph.D degree from Katholieke Universiteit Leuven at 1989 and then worked as a postdoctoral research fellow at K.U. Leuven. In 1991, he joined National University of Singapore and became a full professor in 2004. His research interests include piezoelectric/ferroelectric materials and energy storage materials (Lithium/Sodium ion battery, Solid-state battery and Supercapacitors).

Dr. Huangwei Zhang is an assistant professor in Department of Mechanical Engineering at National University of Singapore. He received bachelor and master degrees in 2007 and 2009 respectively from Beihang University. He worked as a research associate in Peking University from 2009 to 2011. He obtained his Ph.D. degree from University of Cambridge in 2015. He then stayed on from 2015 to 2017 at Cambridge to take up a postdoctoral researcher position. His research covers energy, thermofluids, as well as thermal management and electrochemistry of lithium-ion batteries. He is the senior member of AIAA and member of The Combustion Institute.

crystalline polymers and the migration of sodium ions is completed by themselves along the tunnels.

Precondition for conductivity in polymer electrolytes is that the sodium salts is present in dissociated sate. The polar groups of the polymers with strong ability to act as electron donor like ethylene oxide (—C—O—C), imide (—NH—) and thiol (—S—), can help dissolve sodium salts in polymer matrices.[46] In polymer-salt complexes, cations have great interactions with solvating units of polymer chains while anions usually have weaker interactions with the polymer host. Therefore, three kinds of interactions exist inside the host polymers, namely cation-polymer interactions, anion-polymer interactions and cation-anion interactions. All these three interactions are crucial to the ionic conductivity.

The ionic conductivity, σ, can be expressed as the reciprocal of ionic resistivity, ρ, which is a function of thickness, l, cross-sectional area, A, and the bulk resistance, R_0, measured between two blocking electrodes Equation (1):

$$\sigma = \frac{1}{\rho} = \frac{l}{R_0 A} \tag{1}$$

It is worth noting that the solid polymers are generally dual-ion conductors, which means not only sodium ions but also anions can transport in polymers. Hence, the cation transference number is used to describe the proportion of the total mobile cations and anions. The effective sodium-ion transference number t^+ is given by Equation (2):

$$t^+ = \frac{\mu^+}{\mu^+ + \mu^-} \tag{2}$$

where μ^+ is the sodium-ion mobility and μ^- is the anion mobility.

The mobility also has a relationship with the ionic conductivity Equation (3) :

$$\sigma = \sum n_i q_i \mu_i \tag{3}$$

where n_i is concentration of the charge carrier, μ_i is the mobility and q_i is the number of charges. For sodium ions, the charge q_i is fixed equaling to $+1$. Hence the number and mobility of sodium ions have a large impact on the ionic conductivity. Owing to not only the interaction between anion and cation, but also the migration of both under the electric field generating by cathode and anode, the number and mobility of cation and anion will be influenced by each other. Thus, the sodium-ion transference number is usually less than 0.5 in SPEs, which is small, leading to an inefficient sodium ion conduction.

In general, two models have been well adapted for the relationship between temperature and ionic conductivity in polymer electrolytes, namely Vogel–Tammann–Fulcher (VTF) and Arrhenius. For the first ion conduction mechanism, it usually exhibits the VFT relationship, as given by Equation (4):

$$\sigma = \sigma_0 T^{-\frac{1}{2}} e^{-\frac{B}{T-T_0}} \tag{4}$$

where σ_0 is the pre-exponential factor, T is the absolute temperature, B is the pseudo-activation energy of the conductivity and T_0 is the reference temperature (generally 50 K below the experimental T_g). This kind of relationship relies on the segmental movement of polymer chains and T_g plays a crucial role.

The other mechanism usually exhibits the Arrhenius temperature variation relationship, as given by Equation (5):

$$\sigma = C e^{-\frac{E_a}{k_B T}} \tag{5}$$

where C is the pre-exponential factor, k_B is the Boltzmann constant and E_a is the activation energy. The activation energy means the energy barrier for the sodium ions migrating from its original site to the adjacent sites. The Arrhenius equation shows the relationship between ionic conductivity and temperature for crystalline materials while the VFT is for amorphous materials.

Polyethylene oxide (PEO), poly(vinylidene fluoride) (PVDF), polyalcohols (PVA), and polyvinylpyrrolidone (PVP), are the most applied polymer matrices. These polymers can in general be combined with many kinds of sodium salts such as sodium perchlorate ($NaClO_4$), sodium trifluoromethanesulfonimide (NaTFSI), sodium bis(fluorosulfonyl)imide (NaFSI), sodium iodide (NaI), and sodium trifluoromethanesulfonate ($NaCF_3SO_3$). Table 1 shows the ionic conductivities of several solid polymer electrolytes for SIBs at specific temperatures.

PEO possessing the ability to complex with alkali salts was first reported in 1973[64] and later in 1988, West et al.[65] reported the performance of PEO–$NaClO_4$ as solid electrolyte for solid state batteries. With the increase of temperature, the ionic conductivity of the PEO–$NaClO_4$ increases and the PEO_{12}–$NaClO_4$ reaches the highest ionic conductivity of 6.5×10^{-4} S cm^{-1} at 80 °C. The reason for the enhancement of the ionic conductivity may be the increased amorphous regions in the PEO. It is widely agreed that the transport of sodium ions in PEO-based polymer electrolytes is related to the movement of segmental chains. The increased temperature helps to enlarge the amorphous region and the movement of segmental chains is then increased. Conductivities of some PEO based electrolytes with sodium salts $NaClO_3$ or $NaClO_4$ are shown in Figure 2. The decrease in the apparent activation energy at high temperatures is associated with heating above the melting temper-

Table 1. Ionic conductivities of several SPEs for SIBs at specific temperatures.

Chemical composition	T [°C]	Ionic conductivity [S cm^{-1}]	Ref.
PEO_{12}—$NaClO_4$	80	6.5×10^{-4}	[15]
PEO_{20}—NaFSI	80	4.1×10^{-4}	[54]
PEO_9—NaTFSI	20	4.5×10^{-6}	[55]
PEO_6—$NaCF_3SO_3$	25	2.5×10^{-6}	[56]
70:30 PVA/NaBr	30	1.362×10^{-6}	[57]
PVA:NaI (70:30)	30	1.02×10^{-5}	[58]
PVP:$NaClO_3$(70:30)	35	9.68×10^{-7}	[59]
PVP:$NaClO_3$(70:30)	30	3.28×10^{-7}	[60]
PVP:$NaNO_3$(94:06)	30	1.21×10^{-5}	[61]
60 PVdF:40 $NaClO_4$	100	7.46×10^{-4}	[62]

ChemSusChem

Review
doi.org/10.1002/cssc.202202152

Chemistry Europe
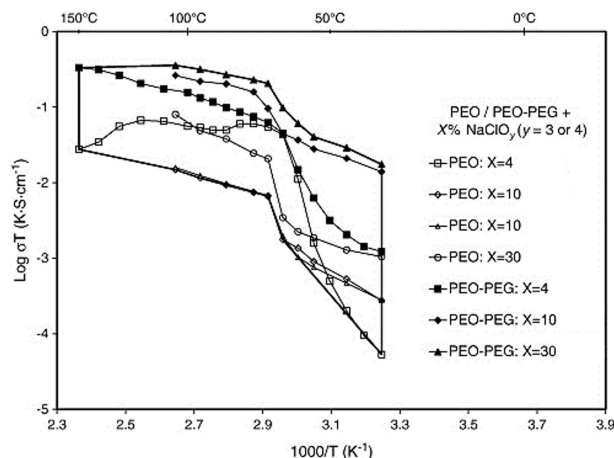European Chemical
Societies Publishing

Figure 2. Conductivities of PEO or PEO—PEG with $NaClO_4$ or $NaClO_3$. Reproduced with permission.[63] Copyright 2012, Elsevier.

ature of PEO. When adding the plasticizer PEG, the sodium ion conductivity at ambient temperature can be increased more than an order of magnitude.

Later, $NaCF_3SO_3$ was also used to add to PEO to investigate its impact on ionic conductivity. Ma et al.[66] found that the concentration of salt in polymer matrix influences the ionic conductivity to a large extent, implying that neither low or high concentrations lead to a decreased conductivity and the specific concentration with highest conductivity is PEO_{20}—$NaCF_3SO_3$ system. The reason for the decrease of ionic conductivity under low concentration is largely because of the small amounts of charge carriers, whereas for the high concentration, it is the consequence of decreased carrier mobility due to chain entanglement. Three years later, PEO—NaTFSI, with greater performance on ionic conductivity compared with the PEO—$NaCF_3SO_3$ system,[67] was reported. This type of anion also has a great influence on ionic conductivity. This high plasticized anion was also reported by Andrea and Patrik[55] from their experimental results from $NaFSI(PEO)_n$ and $NaTFSI(PEO)_n$ systems (n is the molar ratios of ether oxygen to sodium) that TFSI-based electrolytes show obviously better ionic conductivity than that of FSI-based electrolytes under room temperature (Figure 3). For the polymer matrix, it is a dual-ion conductor. Therefore, not only the cations but also the anions have a great impact on ionic conductivity. The superior plasticizing property of $TFSI^-$ anion benefits from its large size and high charge delocalization degree. The weak anion-cation interaction also leads to its high dissociation in PEO. All of these contribute to the high ionic conductivity for $TFSI^-$ based electrolytes under room temperature.

3. Ion Conduction in Ceramics

Inorganic solid electrolytes usually exhibit high ionic conductivity, high ionic mobility, good mechanical properties, and good thermal stability compared to solid polymer electrolytes.[68]
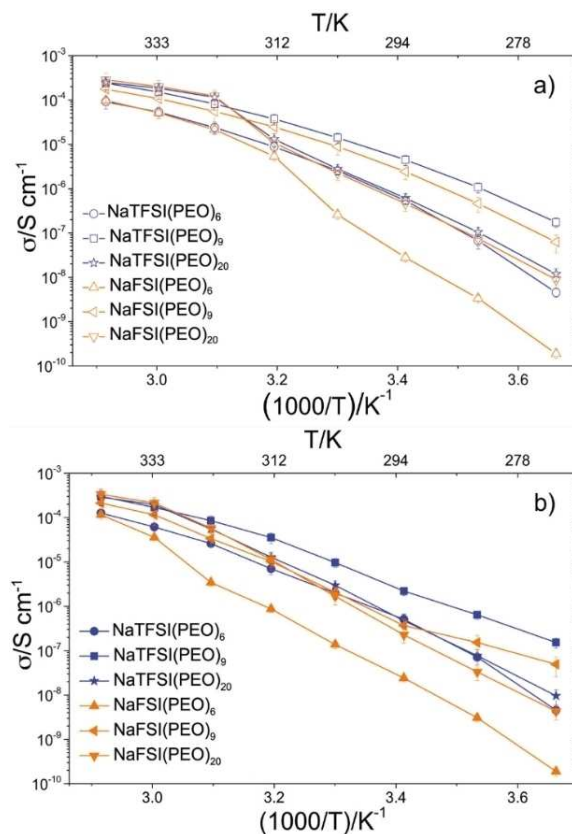

Figure 3. Arrhenius plots of ionic conductivities for $NaTFSI(PEO)_n$ and $NaFSI(PEO)_n$: a) cooling and b) heating scans. Reproduced with permission.[55] Copyright 2015, Elsevier.

Generally, an inorganic crystal has such a structure with defects that serves for ionic transport within the framework. Defects chemistry plays an important role in explaining how the sodium ions transport in these sodium ion conductors. Crystal defects are related to the free energy of the material system. The standard free energy relation is given by Equation (6):

$$\Delta G = \Delta H - T\Delta S \qquad (6)$$

where G is Gibbs free energy, H is the enthalpy, S is the entropy and T is the absolute temperature. The formation of vacancies is caused by entropy. In an ideal state, there should be no vacancies in a perfect crystal at $T = 0$, when the Gibbs free energy of the system has only the contribution of enthalpy. However, when the system is at a certain temperature $T > 0$ K, the thermal vibration of atoms is enhanced, and the enthalpy of the system is increased. When the atom has enough vibration energy to make the amplitude reach a certain limit, it is possible to overcome the constraints of the surrounding atoms, jump away from the equilibrium position, and form a vacancy. This is also to reduce the energy of the system, so a certain number of vacancies will form (driven by the thermal vibrations of the atoms) at temperatures above 0 K. Considering a perfect crystal with N atoms that forms n_V vacancy defects due to thermal

ChemSusChem

Review
doi.org/10.1002/cssc.202202152

Chemistry
Europe
European Chemical
Societies Publishing

excitation. The equilibrium of the defects should satisfy the following relation:

$$\Delta G = n_v(\Delta H - T\Delta S_{vib}) - T\Delta S_{conf} \qquad (7)$$

where ΔG is the change in Gibbs energy, ΔH is the enthalpy of formation of each vacancy, n_V is the number of vacancies, ΔS_{vib} is the vibrational entropy and ΔS_{conf} is the configurational entropy.

There are three kinds of sodium ion transportation mechanisms based on the principle of ionic diffusion (Figure 4).[69] The first kind is a stable sodium ion jumps into an adjacent vacancy site and the second kind is a metastable sodium ion directly jumps to the interstitial site which is not fully occupied. Whereas the third kind is a little complex, a metastable sodium ion replaces a neighboring sodium ion in stable site, and then the replaced sodium ion jumps to an adjacent metastable site, which is called interstitial-substitutional exchange. They can all be explained by the Schottky and Frenkel defects. The relationship between ionic conductivity and temperature in crystalline materials obeys the Arrhenius equation (Equation (5)), it can be derived that the ionic conductivity is related to three parameters, namely the diffusion energy barrier, temperature, and pre-exponential factor (including the amount of sodium ions and available vacancy sites).

Polycrystalline ISEs are comprised of grains and grain boundaries, both of which have strong effect on ionic conductivity. In a general way, sodium ions have to migrate in the grain bulk and transport across grain boundaries. Grain boundary 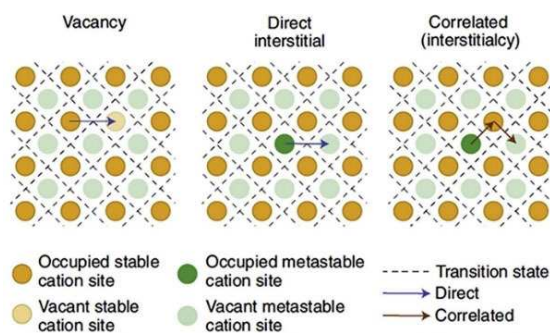is one kind of planar defect arising from mismatching interfaces between adjacent grains. There are abundant point defects with charge which repulse same charged carriers around inside the grain boundaries, resulting in the formation of space-charge layers on both sides shown in Figure 5.[71] Owing to the charge repulsion, there will be a difference in charge carrier concentration between grain and grain boundary. Small number of carriers leads to harder ionic conduction across the grain boundaries than in the grain. Hence, the grain boundaries have a negative impact on the ionic conductivity.

3.1. Beta-alumina

Beta-alumina seems to be the earliest inorganic solid electrolyte discovered for SIBs. In 1967, it was discovered and quickly gained much attention for its high ionic conductivity and excellent thermal stability.[72] The world's first commercial solid-state sodium battery was the high temperature Na–S one using beta-alumina as electrolyte. Beta-alumina is an inorganic layered compound with alternating stacked conduction planes and spinel blocks, and has two different crystal structures, namely β-Al_2O_3 and β''-Al_2O_3 (Figure 6a). The β and β'' phase differ in chemical composition and the order of oxygen atoms stacking in spinel blocks. β-Al_2O_3 has a hexagonal structure and a stoichiometry of $Na_2O(8–11)Al_2O_3$, while β''-Al_2O_3 has a rhombohedral structure and a stoichiometry of $Na_2O(5–7)Al_2O_3$. From the composition, there are more sodium content of β''-Al_2O_3 than β-Al_2O_3, which means that β''-Al_2O_3 has more mobile sodium ions in the conduction plane.[34] Therefore, β''-Al_2O_3 exhibits a higher ionic conductivity of about 2×10^{-3} S cm^{-1}. The conduction of sodium ions in beta-alumina is completed by the ion migration in the conduction plane. It is worth mentioning that single crystal beta-alumina generally exhibits much higher ionic conductivity than polycrystalline beta-alumina, which is highly ascribed to the absence of grain boundaries.[31] Although β''-Al_2O_3 exhibits a high ionic conductivity, it is hard to prepare due to the formation of impurities under high temperature. To obtain purer β''-Al_2O_3, Li$^+$,[73–75] Mg^{2+},[76–78] Ni^{2+},[79] Zr^{2+},[80,81] and Ti^{4+}[82] have been doped as stabilizers. Figure 6b shows the temperature dependence of the ionic conductivities of polycrystalline β-Al_2O_3 and β''-Al_2O_3 with different kinds of stabilizers, which are all Arrhenius temperature variation.

Figure 4. Three kinds of cation migration mechanisms in crystals. Reproduced with permission.[70] Copyright 2022, Elsevier.
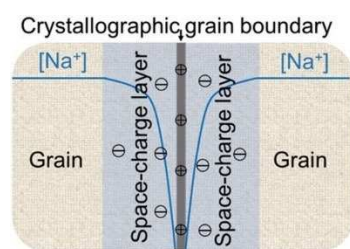

Figure 5. The space-charge layer model of electrical grain boundaries. Reproduced with permission.[71] Copyright 2020, John Wiley and Sons.

3.2. Phosphates NASICON

NASICON stands for sodium (Na) Super Ionic CONductor.[84] Unlike beta-alumina, NASICON is not a layer-structured material but a 3D skeleton with three-dimensional channels for fast sodium ion migration. It was firstly reported by Goodenough's group in 1976 and has a stoichiometry of $Na_{1+x}Zr_2Si_xP_{3-x}O_{12}$ ($0 \leq x \leq 3$, NZSP).[85] NZSP can be considered as the P^{5+} sites in $NaZr_2P_3O_{12}$ are partially substituted by Si^{4+}. When x equals to 2, $Na_3Zr_2Si_2PO_{12}$ shows the highest ionic conductivity. The most widely investigated NASICON structure is $Na_3Zr_2Si_2PO_{12}$, which possibly has two phases, namely rhombohedral and monoclinic (Figure 7a).[30] Both two phases are composed of SiO_4/PO_4

ChemSusChem
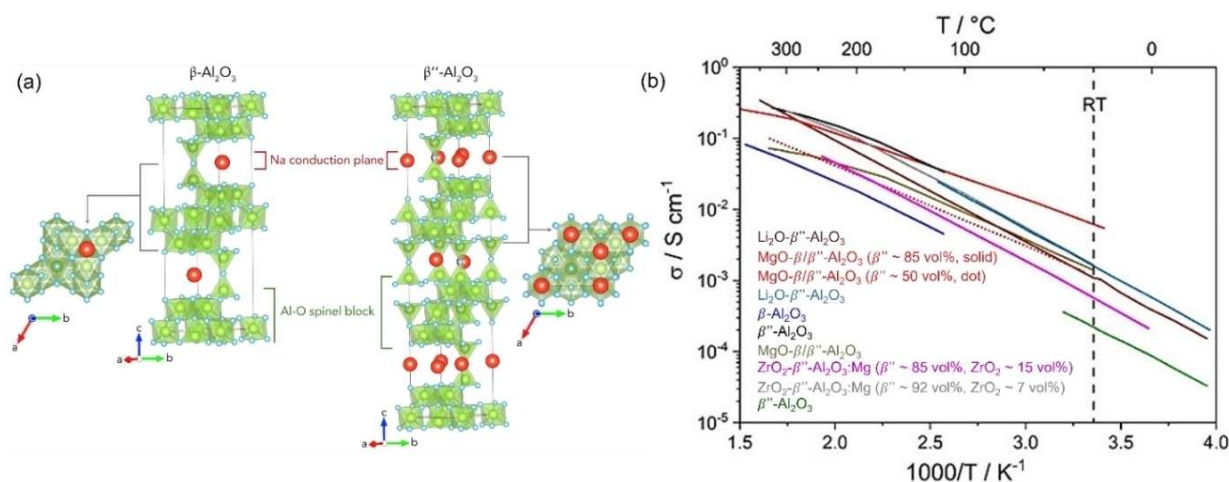
Review
doi.org/10.1002/cssc.202202152

Chemistry
Europe
European Chemical
Societies Publishing

Figure 6. (a) Crystal structures of β-Al$_2$O$_3$ and β″-Al$_2$O$_3$. Reproduced with permission.[30] Copyright 2018, Elsevier. (b) Temperature dependence of the total ionic conductivity of different polycrystalline β/β″-alumina materials stabilized with different elements. Reproduced with permission.[83] Copyright 2020, John Wiley and Sons.
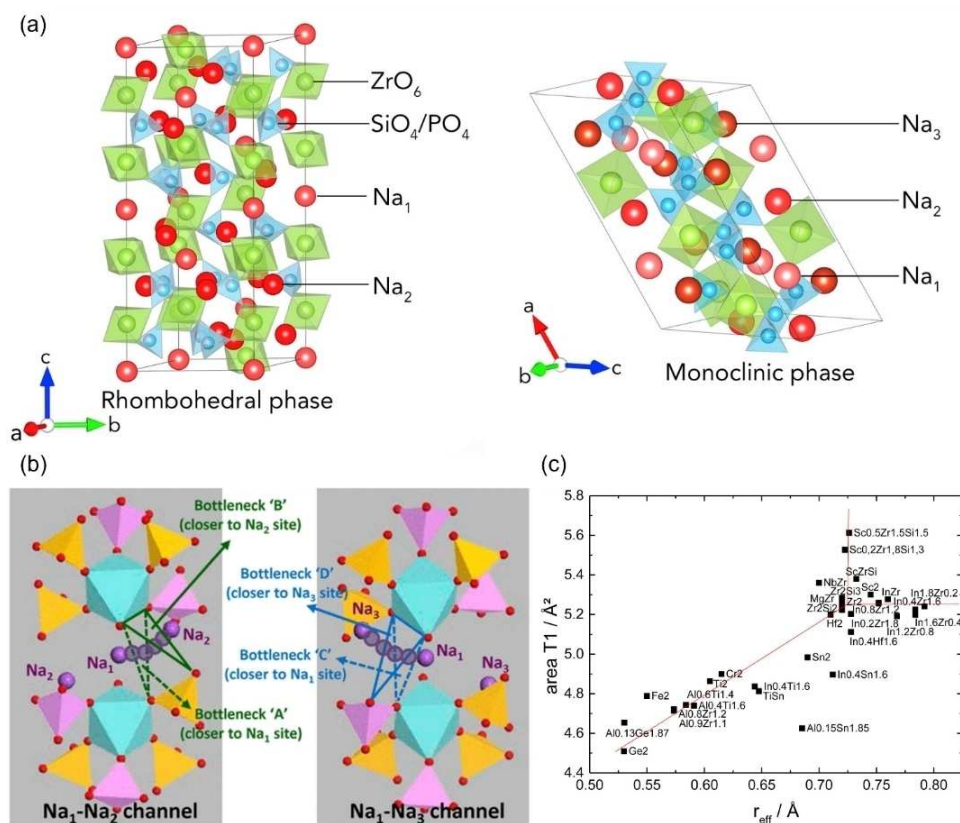

Figure 7. (a) Crystal structures of rhombohedral and monoclinic phase NASICON (Na$_3$Zr$_2$Si$_2$PO$_{12}$). Reproduced with permission.[30] Copyright 2018, Elsevier. (b) Four different types of bottlenecks (A–D) in Na-conducting pathways in the monoclinic NASICON structure. Reproduced with permission.[86] Copyright 2016, American Chemical Society. (c) Dependence of the triangle area on the effective ionic radius. The lines are a guide to the eye. Reproduced with permission.[91] Copyright 2015, Elsevier.

tetrahedra and ZrO$_6$ octahedra with corner-sharing oxygen atoms. There are four sodium sites in both rhombohedral and monoclinic phases, but they occupy different sites. For the monoclinic, there are four sites, namely one Na$_1$, two Na$_2$ and one Na$_3$, whereas there are only one Na$_1$ but three Na$_2$ in rhombohedral. The migration of sodium ions is completed by going through bottlenecks of which the size determines the migration energy barrier of the sodium ions. There are four

ChemSusChem

Review
doi.org/10.1002/cssc.202202152

**Chemistry
Europe**
European Chemical
Societies Publishing

different kinds of bottlenecks in monoclinic phase, which are two Na_1–Na_2 and two Na_1–Na_3 channels (Figure 7b).[86] For the rhombohedral phase, there are just two bottlenecks for sodium ion transportation. The migration of sodium ions is completed by the movement from Na_1 site to Na_2 site nearby via mid-Na position. Because the size of bottlenecks has a great impact on the ionic conductivity, the common method to improve ionic conductivity is doping alkaline earth ions like Mg^{2+},[87] La^{3+},[88,89] and Sc^{3+}[90] to enlarge the bottleneck size. There is an optimal ionic radius for the doping cations (Figure 7c), which is near 0.72 Å.[91] Doping is used to increase ionic conductivity in bulk, but sodium ions migrate across the grain boundaries, which also affects the ionic conductivity. Increasing the grain size also means decreasing the amounts of grain boundaries, which can enhance the ionic conductivity.

3.3. Sulfides

Previous studies have already reported the possibility that sulfide-based SSEs become alternatives for oxide-based SSEs.

Compared with oxide-based SSEs, the sulfide-base SSEs exhibit a higher ionic conductivity in the room temperature due to the larger atomic radius of sulfur than oxygen, resulting in a smaller electronegativity and a decreased electrostatic force between sodium ions and sulfur atoms. Therefore, the migration of sodium ions is easier and faster in sulfide-based SSEs. The most widely investigated sulfide-based SSE Na_3PS_4 reported in 1992 has two crystal structures shown in Figure 8a,[92] which are tetragonal and cubic and both of whose ionic conductivities are too low for practical application. The general existing phase of Na_3PS_4 is tetragonal but can transform to cubic phase at high temperature. The lattice difference between these two phases is very small only about 0.01 nm. There are two sodium sites in the tetragonal phase both of which are fully occupied, whereas there is only one kind of fully occupied sodium site in cubic phases. Despite the single Na_1 site, the sodium ions are proved to be mobile and can move from its original site to the adjacent sodium sites. Until 2010s, glass-ceramic sulfide electrolyte discovered by Hayashi et al.[93] with a high ionic conductivity of 2×10^{-4} S cm^{-1} promoted the development of sulfide-based SSEs applied for SIBs. The most efficient method to enhance the
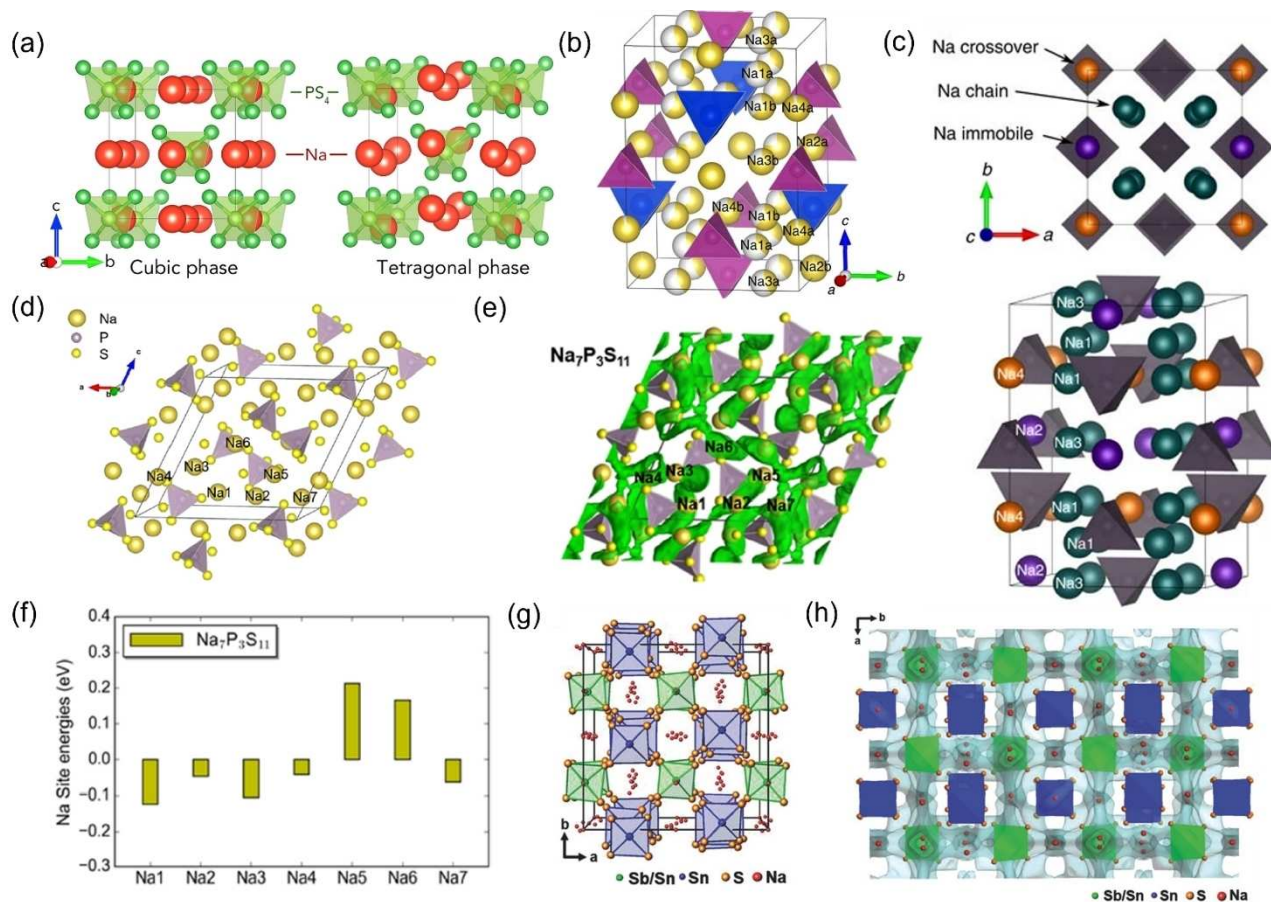

Figure 8. (a) Crystal structures of cubic and tetragonal phase Na_3PS_4. Reproduced with permission.[30] Copyright 2018, Elsevier. (b) Structure of $Na_{10}SnP_2S_{12}$ from DFT calculations. (c) Illustration of the Na-chain, Na-crossover, and Na-immobile sites; gray tetrahedra represent SnS_4 and PS_4; all spheres are Na sites. Reproduced with permission.[96] Copyright 2016, Springer Nature. (d) Calculated crystal structure of $Na_7P_3S_{11}$; (e) Calculated Na-ion probability densities in $Na_7P_3S_{11}$; (f) Na site energies in $Na_7P_3S_{11}$. Reproduced with permission.[97] Copyright 2017, American Chemical Society. (g) Crystal structure of $Na_{3.75}Sn_{0.75}Sb_{0.25}S_4$ from (001) view. (h) 3D bond valence difference map isosurfaces for $Na_{3.75}Sn_{0.75}Sb_{0.25}S_4$. Reproduced with permission.[98] Copyright 2018, John Wiley and Sons.

ChemSusChem

Review
doi.org/10.1002/cssc.202202152

**Chemistry
Europe**
European Chemical
Societies Publishing

ionic conductivity of Na_3PS_4 is to introduce defects like sodium interstitial and vacancies.

In 2015, $Na_{10}GeP_2S_{12}$ was predicted via first-principles simulations with a crystal structure same as $Li_{10}GeP_2S_{12}$.[94,95] The crystal structure of $Na_{10}GeP_2S_{12}$ is composed of sodium ions together with GeS_4 and PS_4 tetrahedron. One year later, another superionic conductor $Na_{10}SnP_2S_{12}$ (Figure 8b) with the same crystal structure as $Na_{10}GeP_2S_{12}$ was synthetized successfully and obtained a relatively high room-temperature ionic conductivity of $0.4\ mS\,cm^{-1}$.[96] There are four sodium sites in $Na_{10}SnP_2S_{12}$ (Figure 8c), two of which belong to the Na-chain sites (Na_1 and Na_3) and the rest two are Na-crossover sites (Na_4) and Na-immobile sites (Na_2).[96] At low temperatures, the energy of the sodium ions occupying the Na-chain and Na-crossover sites are almost the same, resulting in a low energy barrier for migration of sodium ions in three dimensions. And that's why $Na_{10}SnP_2S_{12}$ has a high ambient ionic conductivity.

$Na_7P_3S_{11}$ is another kind of sulfide-based solid electrolytes, which was also derived from a lithium superionic conductor $Li_7P_3S_{11}$. It was also developed via first-principles computational technique.[97] The as-calculated crystal structure of $Na_7P_3S_{11}$ is shown in Figure 8d, composed of sodium ions and PS_4 tetrahedron. Through the analysis on the distribution of sodium ions, the ion conduction in $Na_7P_3S_{11}$ is completed by a three-dimensional diffusion network, which means all seven sodium sites are connected to each other. From the result of probability density analysis (Figure 8e), sodium ions are distributed evenly, resulting in a relatively flat energy landscape along the channels. The as-calculated energy of sodium sites (Na_1–Na_7) shown in Figure 8f also indicate the easy migration for sodium ions among these sites.

As many sulfide-based electrolyte contain phosphorus, which leads to poor chemical stability, a new kind of sulfide $Na_{4-x}Sn_{1-x}Sb_xS_4$ ($0.02 \leq x \leq 0.33$) was developed.[98] When $x = 0.25$, this kind of structure has the least impurity phase of $3.4\ wt\%\ Na_3SbS_4$. The crystal structure of $Na_{3.75}Sn_{0.75}Sb_{0.25}S_4$ from (001) view is presented in Figure 8g. There are one tin site, one antimony/tin mixed site, three sulfur sites, and five sodium sites in the unit cell. All sodium sites are not fully occupied with an average vacancy of 6.3%, providing vacancies for sodium ions to migrate. Although the crystal structure of $Na_{3.75}Sn_{0.75}Sb_{0.25}S_4$ is complex, the interatomic distances between adjacent sodium sites are limited in a range of 3.42–3.53 Å. 3D bond-valence sum mappings (BVSM) were used to prove that $Na_{3.75}Sn_{0.75}Sb_{0.25}S_4$ has 3D-dimentional fast ion conduction pathways. The 3D bond valence difference map isosurfaces of $Na_{3.75}Sn_{0.75}Sb_{0.25}S_4$ are shown in Figure 8h, from which the possible sodium-ion diffusion pathways are clearly presented. The fast ion conduction in 3D pathways inside $Na_{3.75}Sn_{0.75}Sb_{0.25}S_4$ account for its high ionic conductivity of 0.2–$0.5\ mS\,cm^{-1}$ at 30 °C.

4. Ion Conduction in Composite Polymer Electrolytes

Although the mainstream research direction has been LIBs since the successful commercialization by SONY in 1991, the development of SIBs has been promoted to some extent, especially the past 20 years, and both SPEs and ISEs have become potential solid electrolytes for all-solid-state SIBs. However, both SPEs and ISEs cannot satisfy the requirements for practical applications for SIBs due to their subsistent disadvantages. ISEs exhibit superior ionic conductivity, thermal and chemical stability but they are very rigid and brittle, which will lead to poor interfacial contact between ISEs and electrodes. SPEs offer a better interfacial contact owing to its great mechanical flexibility. Nonetheless, their unsatisfactory room-temperature ionic conductivity, thermal stability, and mechanical strength impede their practical application. From the fabrication perspective, SPEs own very easy fabrication processes like solution casting, in situ polymerization and UV curing, which are all very economical. While the sintering of ISEs often requires very high temperature with large amounts of energy consuming. Moreover, compared with ISEs, the main advantage of SPEs is joining of the cell components and battery assembly. Many strategies have been applied to improve the performance of ISEs and SPEs, but still cannot reach the target for practical application. To some extent, ISEs and SPEs are complementary each other.

Design of electrolytes via combination of polymer and ceramics to form a new class of composite polymer electrolytes (CPEs) follows two different approaches. The first kind is polymer-ceramic composites with sodium-ion conductive polymer and non-conductive ceramic components. The advantages of the addition of passive ceramic particles into the polymer are: (i) modifying the properties of the polymer matrix via interactions between the polymer and the ceramic particles to decrease the crystallinity of polymer matrix for enhancement of sodium-ion conductivity; and (ii) improving the mechanical properties of the polymer matrix. The second kind is also polymer-ceramic composites, consisting of both sodium-ion conductive polymers and sodium-ion conductive ceramics. The addition of active ceramics resulting in three advantages: (i) enhancing the overall ionic conductivity by introducing an active ceramic component with higher ionic conductivity than the polymer; (ii) improving the ionic conductivity by decreasing the crystallinity of the polymer in regions adjacent to the ceramic particles; and (iii) strengthening the mechanical properties of the whole electrolyte.

The chemical interactions between the polymer matrix and the ceramic particles are governed to a large part by the surface termination of the ceramic particles. Lewis acid and Lewis base characteristics of the surface termination lead to different adsorption (bonding) states on the polymer/ceramic interfaces. Based on the Lewis acid-bases theory, there are many kinds of Lewis acid and base centers existing in composite polymer electrolyte systems. And the final structure and performance of CPEs are determined by the equilibrium between various Lewis acid-base reactions.[99] It is worth mentioning that Lewis acid-

ChemSusChem

Review
doi.org/10.1002/cssc.202202152

**Chemistry
Europe**
European Chemical
Societies Publishing

base interactions help the dissociation of sodium salts in the interface region formed between the polymer and the ceramic.[100] Simulations also have proved that there is an interfacial area formed between the bulk polymer phases and the single ceramic particles, in which the disorder of the polymer chains increases, resulting in an enhanced dissociation of salts and an improvement of ionic conductivity.[101]

Considering the polymer-passive ceramic CPEs, the impact of the local regions of enhanced conductivity on the overall sodium-ion conductivity depends on at least three parameters, which are the (radial) extension of the zone with enhanced conductivity in the surface formed by polymer and ceramic, the size of the particles and the volume fraction of the ceramic particles (Figure 9). In materials with small extension of the region with enhanced ionic conductivity and low volume fractions of the ceramic particles, the regions of the enhanced ionic conductivity remain well separated, so the impact on the overall ionic conductivity will be limited. This holds for small as well as large particle size (Figure 9a, b). Along with wider zones of the enhanced ionic conductivity (Figure 9c) or larger volume fractions of the ceramic particles (Figure 9d), the regions of the enhanced conductivities stemming from the interactions with the individual particles overlap and provide percolating high conduction pathways. However, in these scenarios, part of the electrolyte volume is blocked by the non-conductive ceramics. The most favorable configuration providing high overall ionic conductivity is characterized by small particles, small volume fractions of non-conductive ceramics but extended regions of disordered and high conductive polymer (Figure 9e).

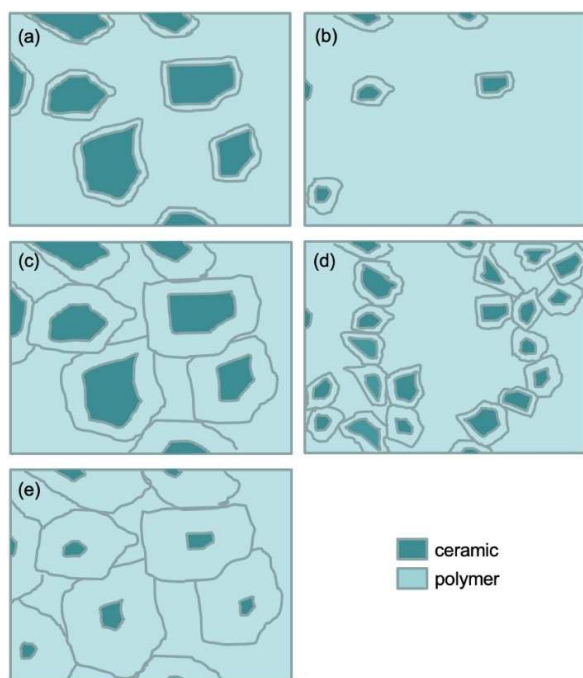Overall, the strategy for the design of the CPEs with non-conductive ceramics can be outlined as maximizing the volume fraction of disordered polymer while ensuring percolation paths of this component using a minimum volume fraction of the non-conductive ceramic component.

The challenge for the design of CPEs with conductive ceramics is more complex and depends, in addition to volume fractions, particle size and zones of the polymer influenced by the ceramics, on the ionic conductivity of the ceramics and the interface resistance between the polymer and the ceramic, which are the two most important features (Figure 10a, c, e). In addition to the sodium-ion conductivities of the polymer and the ceramic components, the enhanced local conductivities of the polymer close to the ceramics, the resistance at the interface between the polymer and the ceramic and, eventually, the resistance between the individual ceramic particles have to be considered.

In case of non-percolating ceramic structures in the CPEs, the most important is the interface resistance along with the transition of the sodium ions between the ceramics to the polymers and vice versa. In case this interface resistance is low, in spite of low volume fractions, large part of the conduction will take place in the ceramic. In contrast, along with high interface resistance, the main conduction will take place in the polymer phase close to the ceramic components, because the sodium ions do not enter the ceramic components. In this case, the maximation of the zones with disordered high-conductive polymer will be the objective. In case the ceramic structures are percolating, the interface resistance on contact between individual ceramic particles has to be determined.

Figure 10 describes three different scenarios of CPEs with different volume fractions of active ceramic components. The first scenario (Figure 10a) is that the amount of ceramics is too small to form a continuous pathway for sodium ions to migrate. And the polymer-ceramic interfaces also cannot connect to each other to form a continuous pathway for sodium ions. The
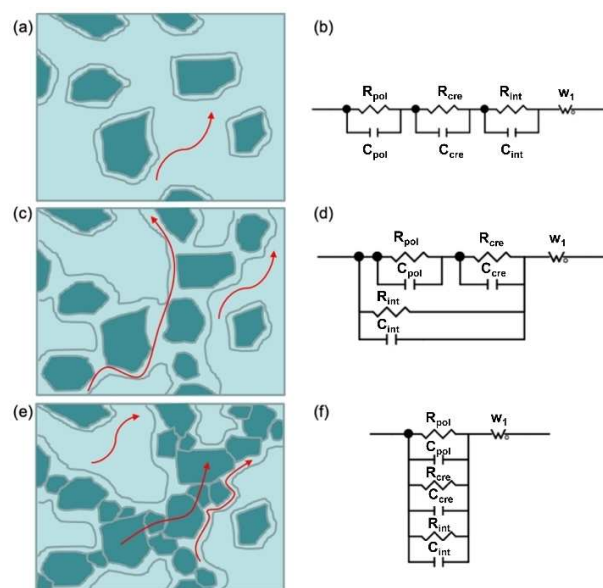

Figure 9. Regions of enhanced Na-ion conductivities along with different microstructure scenarios.

Figure 10. Three scenarios of CPEs with different ceramic volume fractions (a, c, e) and equivalent circuits for each scenario (b, d, f).

ceramic particles just plasticize the local region of polymer matrix and sodium ions can only migrate in the polymer matrix, which will lead to a low-sufficient sodium ion transport. Therefore, the three components, the polymer, the ceramic and the interface, are all playing their role separately; the equivalent circuit can be expressed as shown in Figure 10b. The second situation (Figure 10c) is that the volume fraction is providential to help form the continuous interface pathways but the ceramic particles still cannot connect to each other to from a continuous pathway for cation migration. As a new fast-ion conduction pathway is formed, the ionic conductivity of the electrolyte will be enhanced a lot. So, the equivalent circuit can be considered as shown in Figure 10d. The volume fraction of ceramics in the last scenario (Figure 10e) is big enough for the formation of continuous pathways between ceramic particles. There are totally three kinds of continuous pathways for sodium ions to migrate. So under this situation, the migration of sodium ions becomes easier. The equivalent circuit under this situation can be considered as shown in Figure 10f.

Therefore, ion conduction in CPEs with active ceramics is more complex than that with passive ceramics for the increase of ion conduction pathways.

4.1. CPEs with passive ceramics

The inert fillers mean that the additive inorganic crystals are unable to conduct sodium ions by themselves. Study from the size effect of ZrO_2 nanoparticles on ionic conductivity added in $PEO-NaClO_4$ matrix demonstrated that the room-temperature ionic conductivity is inversely proportional to the particle size.[102] The addition of ZrO_2 nanoparticles decreases the crystallinity of PEO polymer, and the increased amorphous region due to the addition of ceramic powders can hence improve the transport of ions due to the easier segmental movement. The effect of SiO_2 addition on ionic conductivity for $PEO-NaHCO_3$ matrices was discussed by Chandra et al.[103] They found that the increase of room-temperature ionic conductivity is owing to the increased number and mobility of free sodium ions shown in Figure 11a. Therefore, it was proposed that the Lewis acid-base reaction enhances the ionic conductivity. Later in 2021, the effect of TiO_2 addition into the PEO–NaI matrices was also investigated[104] and it was noted that three factors account for the enhancement of ionic conductivity due to the added TiO_2, which are increased amorphous degree, Lewis acid-base reaction and newly built sodium ion conduction pathways. The Lewis acid-base reaction is due to the interaction between the polar surface groups of ceramic filler and polymer matrix, which create new pathways and migration sites for sodium ion conduction.[105,106] Generally, the addition of ceramic powders favors the decrease of crystalline phase and increase the amorphous phase which is good for the enhancement of ionic conductivity.

Another worth-mentioned point is that the addition of ceramics provides more ion conduction pathways to the increase of ionic conductivity. However, an otherwise was reported that the ceramic addition does not change the ionic
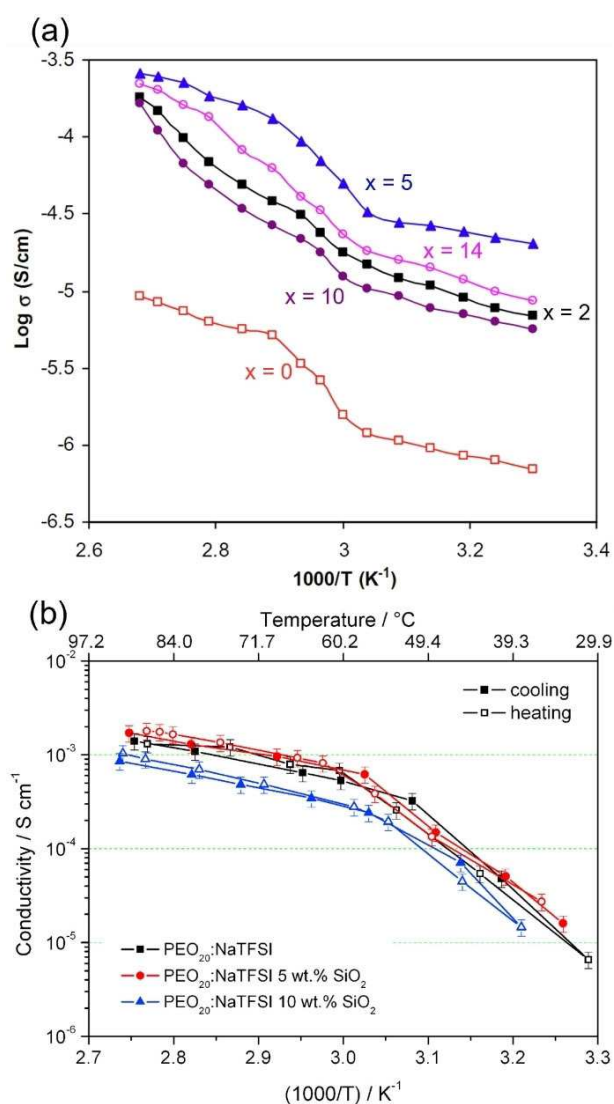

Figure 11. (a) Arrhenius plots for hot-pressed NCPEs: $(100-x)[70PEO:30NaHCO_3]+xSiO_2$, where $x=0$, 2, 5, 10, 14 wt%. Reproduced with permission.[103] Copyright 2016, Elsevier. (b) Conductivity Arrhenius plots of the $EO:NaTFSI=20:1$ membranes with 0, 5% or 10% of silica on heating and cooling scans. Reproduced with permission.[107] Copyright 2014, Elsevier.

conductivity obviously.[107] The experiment conducted was carried out by adding SiO_2 into the PEO–NaTFSI matrices followed by electrochemical impedance test. The results shown in Figure 11b indicate that the addition of SiO_2 has no obvious effect on the enhancement of ionic conductivity. On the contrary, too much ceramic powder added led to a reduced ionic conductivity due highly to the ceramic agglomeration. This wield phenomenon is arising from the high plasticizing ability of the $TFSI^-$ anion. The high plasticizing effect will cover the SiO_2 effect acting on ionic conductivity. This also reflects the complexity of ion conduction in CPEs, because there are multiple ion conduction pathways, and these factors will affect each other. Despite the complexity of ion conduction mecha-

nism, the addition of ceramic fillers improves the mechanical strength of solid polymer electrolytes.

4.2. CPEs with active ceramics

Yao et al.[108] fabricated SPEs by adding beta-alumina filler into the PEO—NaClO4 matrices and discovered the effect of addition of beta-alumina on the ionic conductivity. There is no doubt that the ionic conductivity of SPE is enhanced with the addition of beta-alumina added (Figure 12a) mainly because of the decreased crystallinity of PEO matrix. From the temperature dependence of ion conductivity plot shown in Figure 12b, the conclusion can be drawn that the improvement of ionic conductivity is weaker at high temperatures than that at room

temperature because at high temperatures, PEO transfers from semi-crystalline to amorphous state, where the movement of segmental chains is more quickly, thus leading to a more and faster sodium ion migration. Therefore, at high temperatures, the amorphous region of PEO acts as the main medium for ion conduction. However, at room temperature, the SPE with filler added shows an obviously higher ionic conductivity than that without filler addition arising from the reduced crystallinity of PEO. Similar to the results shown above, the addition of beta-alumina ceramic fillers is also limited to about 10% to obtain a highest ionic conductivity (Figure 12c). Despite the importance in the enhancement of ionic conductivity of SPEs due to the amorphous region, the newly formed fast-ion conduction pathways in the interface between active filler and polymer also serve an indispensable role. It was proposed that the interface
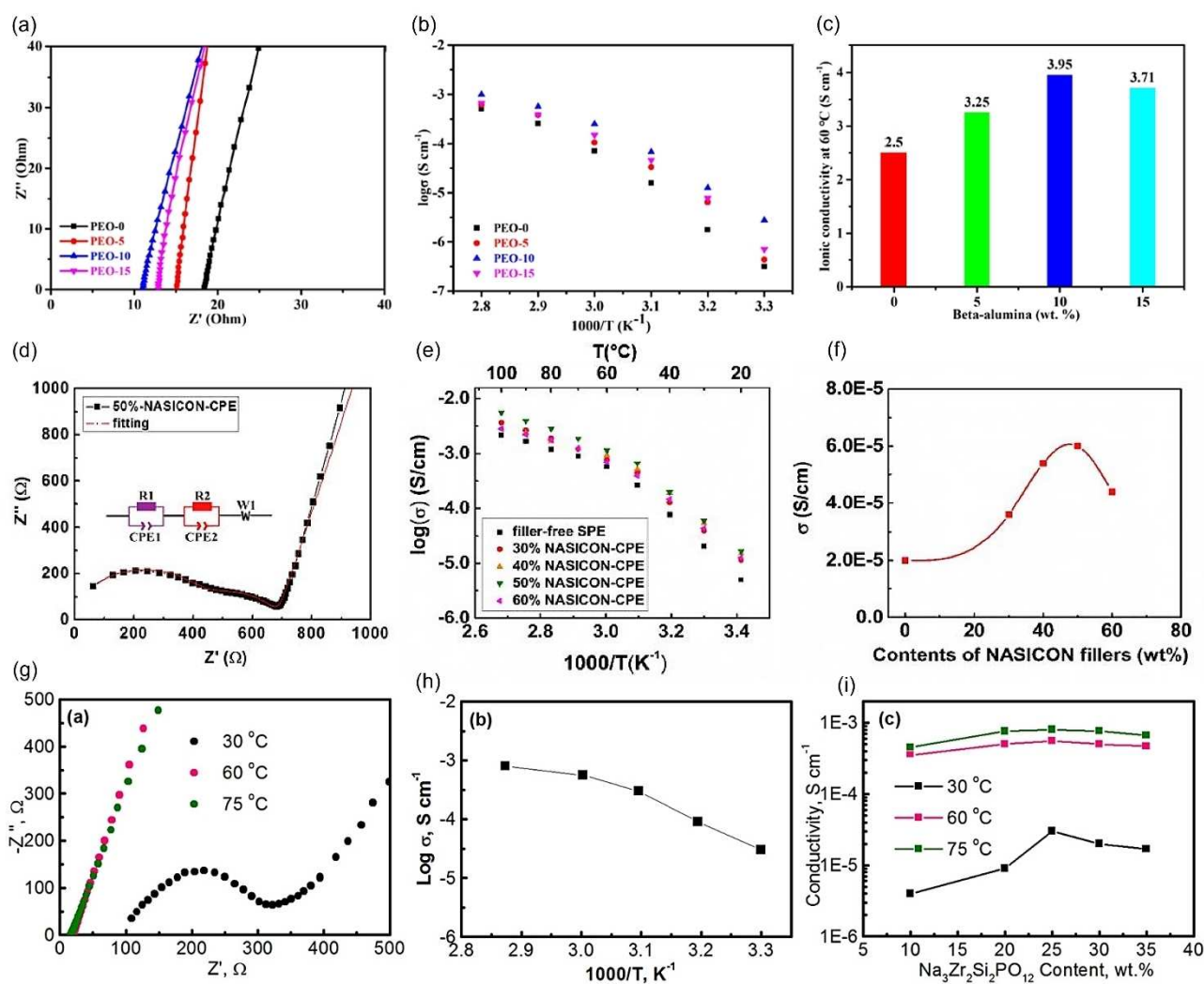

Figure 12. (a) Nyquist curves, (b) temperature dependence of ionic conductivity, at 60 °C when the addition amount of beta-alumina is 10 wt%; (c) The ionic conductivity of CPEs with different beta-alumina compositions at 60 °C. Reproduced with permission.[108] Copyright 2021, Springer Nature. (d) The impedance spectra of the 50 wt% NASICON-CPE at 25 °C with the equivalent circuit employed to fit the data; (e) The temperature dependence conductivities of the NASICON-CPEs over a temperature range of 20–100 °C; (f) The ionic conductivity of NASICON-CPEs with different compositions at 30 °C. Reproduced with permission.[109] Copyright 2017, Elsevier. (g) Nyquist plots of the electrochemical impedance spectroscopy of the PEO—NaClO4—Na3Zr2Si2PO12 membranes (with 25% Na3Zr2Si2PO12) at different temperatures; (h) Arrhenius plots of the PEO—NaClO4—Na3Zr2Si2PO12 membranes (with 25% Na3Zr2Si2PO12); (i) Ionic conductivities of the PEO—NaClO4—Na3Zr2Si2PO12 membranes with different contents of Na3Zr2Si2PO12 at different temperatures. Reproduced with permission.[110] Copyright 2019, American Chemical Society.

ChemSusChem

Review
doi.org/10.1002/cssc.202202152

Chemistry
Europe

European Chemical
Societies Publishing

between active filler and polymer matrix is a fast ion transport channel formed in the composite polymer electrolytes.

In addition to nonactive fillers used, the effects of active fillers such as NASICON in the PEO–NaTFSI matrix firstly were investigated.[109] From the experimental results, the addition of NASICON powders enhanced the thermal and electrochemical stability of CPEs and exhibited a high ionic conductivity of 2.8 mS cm^{-1} at 80 °C. Compared with the above mentioned nonactive ceramic filler content, the content of NZSP in this study reached a relatively high amount of about 50 % (Figure 12e, f). It is commonly accepted that the content of inert fillers has an optimal proportion, which is usually less than 15 %. This is because that large amounts of inert fillers will agglomerate and they do not conduct sodium ions by themselves, too many inert fillers will impede the migration of sodium ions. Different with inert fillers, active fillers can account for a larger part of CPEs than inert fillers for their own abilities to conduct sodium ions. Figure 12d shows the Nyquist spectra of PEO$_{14}$–NaTFSI and PEO$_{14}$–NaTFSI–50%NZSP and the obvious difference is that the filler-free CPE only gives rise to one semicircle, whereas there are two semicircles for NZSP-CPE. The high-frequency semicircle indicates the ion migration between ceramic grains or the polymer-ceramic interface because both two transportations are finished by fast ion-conduction pathways while the low-frequency semicircle is supposed to belong to the ion motion in the polymer matrix exhibiting slower ion conduction speed. Therefore, four assumptions for the enhanced ionic conductivity were conducted. They are that (i) the active filler, namely NZSP, decreases the crystalline of PEO matrix and hence increases the movement of segmental polymer chains, (ii) the introduction of the NZSP forms new sodium ion migration channels which is the interface between PEO and NZSP caused by the percolation effect, (iii) since there is sodium ion concentration gradient between polymer matrix and ceramic filler, the sodium ions in high-concentration NZSP can diffuse to low-concentration polymer matrix resulting in more sodium vacancies on the surface of NZSP, and more sodium vacancies provide more sites for sodium ion migration and lead to a higher ionic conductivity, and (iv) the active ceramic itself is a fast-ion conductor, so that the total ionic conductivity is enhanced due to the addition of NZSP fillers. Therefore, the combination of ISEs and SPEs as CPEs has a great meaning to become next-generation novel solid polymer electrolytes.

Yu et al.[110] also fabricated one kind of PEO–NaClO$_4$–Na$_3$Zr$_2$Si$_2$PO$_{12}$ CPE. From the Nyquist plot (Figure 12g), at 30 °C, there is an obvious semicircle at high frequency. When temperature is over 60 °C, the semicircle disappears. This is because when the temperature increases, the charges stored in the grain boundaries become less and the polymers transform from semi-crystal to amorphous phase, resulting in a smaller interfacial impedance and charge transfer impedance. Firstly, with the increase of temperature especially when it is higher than the melting point of polymer matrix, polymer become amorphous and the ionic conductivity should increase. Another possibility is that with the temperature increases, the interface between polymer and ceramic becomes

better and the resistance is eliminated. NZSP and PEO are two totally different phases so that it is normal that there is an interface between them. It is also noted that the ionic conductivity has a great jump from 30 °C to 60 °C mainly because of the melt of the polymer matrix (Figure 12h), leading to whole PEO becoming amorphous. Another important point is that when the temperature increases, the role of NZSP becomes inconspicuous. The ionic conductivities of NZSP content between 20 % to 30 % are very close to each other at high temperatures (Figure 12i), which means the main factor enhancing ionic conductivity is the amorphous phase of PEO. This also proves that the ion conduction happens mainly in the amorphous phase. However, at about room temperature, the crystallinity of polymer matrix is relatively high where the NZSP can play an important role in decreasing the crystallinity. This does not mean that the more NZSP content, the higher the ionic conductivity. When the ceramic content is over 25 %, the ionic conductivity measured at 30 °C decreases due to the agglomeration of ceramics. Despite of the complexity of the ion conduction of the CPE due to many factors, there are several common recognitions for enhancement of ionic conductivity, such as decreasing the crystallinity of polymer matrix and creation of ion pathways between the ceramics and polymer matrix.

The sulfide-based ceramics were also added into the polymer-salt matrix to investigate their performance in the enhancement of ionic conductivity.[111] Lu et al. fabricated one kind of CPE composed of PEO polymer matrix, NaTFSI and Na$_3$SbS$_4$ ceramics. The optimal Na$_3$SbS$_4$ weight ratio is 25 wt% of PEO, affording a room-temperature ionic conductivity of 2.47×10^{-5} S cm^{-1} (Figure 13a). From Figure 13b, it is clear that, with the addition of Na$_3$SbS$_4$, the ionic conductivity of the as-fabricated electrolyte enhanced an order of magnitude. The reasons why the ionic conductivity is improved are not only the addition of Na$_3$SbS$_4$ decreases the crystallinity of PEO matrix and Na$_3$SbS$_4$ itself owns a superior ionic conductivity, but also the interactions between components in the as-fabricated electrolyte. In virtue of characterization techniques, the possible interactions inside the electrolyte can be revealed. There are four kinds of interactions exist (Figure 13c). First of all, there are interactions between Na$_3$SbS$_4$ and TFSI$^-$, which improve the sodium ion transference number and promote the dissociation of sodium salts. Then, the interactions between Na$_3$SbS$_4$ and PEO will form an interface which is considered as a fast sodium ion conduction pathway. The third interaction exist between PEO and sodium ions, this is because the PEO matrix has the ability to dissolve sodium ions. And the last interaction is between anion and cation due to the electrostatic interaction.

One means to form a fast ion-conduction pathway is through fabrication of a 3D porous NZSP framework with continuous PEO–NaTFSI filler (Figure 14c).[112] This 3D CPE exhibits an excellent ionic conductivity of 1.4×10^{-4} S cm^{-1} at room temperature. The reason for the high ionic conductivity is due highly to a porous but continuous 3D NZSP framework, resulting in continuous fast ion conduction pathways. Unlike other ceramic powders used in most CPEs, Wang proposed a successful synthesis of porous but continuous 3D NZSP ceramic
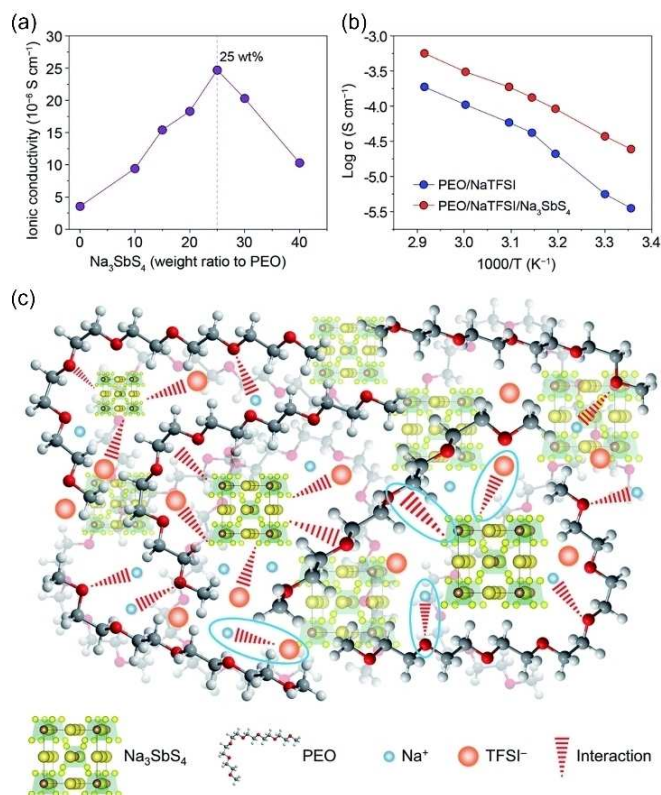
ChemSusChem

Review
doi.org/10.1002/cssc.202202152

Chemistry Europe
European Chemical
Societies Publishing

Figure 13. (a) Ionic conductivity of the electrolyte with different contents of Na_3SbS_4 (calculated based on the mass of PEO). (b) Ionic conductivity of pristine PEO–NaTFSI electrolyte and PEO–NaTFSI–Na_3SbS_4 electrolyte at different temperatures. (c) Schematic diagram of the structure of the PEO–NaTFSI–Na_3SbS_4 electrolyte, where the four types of interactions between different components are highlighted. Reproduced with permission.[111] Copyright 2022, Royal Society of Chemistry.

framework, then PEO–NaTFSI was infiltrated into the framework. As the NZSP framework is rigid while the PEO–NaTFSI filler is flexible, the pores of the NZSP can be filled with PEO–NaTFSI. Owing to the special structure of the NZSP, there are many continuous interfaces between PEO and NZSP, which accounts for the high ionic conductivity, which is higher than the pre-reported PEO-based electrolytes shown in Figure 14d. The Atomic Force Microscope (AFM) was applied for the investigation of sodium ion migration at the well-built NZSP-PEO/NaTFSI interface. The results showed that the fastest ion conduction appeared at the interface rather than individual NZSP or PEO, and this is the first time to realize the direct presentation of fast ion diffusion at NZSP-PEO/NaTFSI interface (Figure 14a and b), which is also a perfect explanation of such a high ionic conductivity under room temperature.

Generally speaking, although the ion conduction mechanism in CPE is complex, several conclusions can still be drawn from the experimental results. The sodium ion conduction is highly considered to happen in the amorphous region of polymer matrices and therefore decrease of the crystallinity of polymer is a method to increase the ionic conductivity. Furthermore, creation of large amounts of continuous interfaces between the organic and inorganic materials is important since

it creates many ion pathways. The last point needs to mention is that the active fillers exhibit much better performances than passive fillers for the active fillers themselves can transport sodium ions while passive fillers cannot conduct sodium ions.

5. Ion Conduction in Composite Gel Polymer Electrolytes

Gel polymer electrolytes (GPEs) for SIBs are usually made of polymer-sodium salt system with little liquid plasticizer or solvent or both.[113] Compared with liquid electrolytes, they can be considered as quasi solid for the much less mobility (Figure 15). The addition of liquid components promotes ionic conductivity than that of pure solid electrolytes. However, Since GPEs also uses polymers, such as PEO, PVDF, PVDF-HFP and PAN as polymer matrices,[114] with the addition of liquid phase, the mechanical strength of the GPEs is usually poor. Therefore, GPEs also need the introduction of inorganic ceramic powders to enhance its mechanical properties for practical application. The composite GPEs is a combination of both LEs and CPEs, hence exhibiting both advantageous of high ionic conductivity from the liquid phase and good mechanical strength due to solid additives.

Hashmi et al.[115] explored the effect of active and passive fillers acting on ionic liquid-based CGPEs. $NaAlO_2$ and Al_2O_3 were used as active and passive filler respectively. The results showed that the addition of both ceramic fillers has a slight improvement on ionic conductivity, but the active filler-based CGPEs show a higher ionic conductivity than passive filler-based CGPEs. This is due to that the active fillers themselves can conduct sodium ions, which provides more ion conduction sites resulting in a higher ionic conductivity. Zhao et al.[116] investigated the performance of PVDF-HFP/SnO_2/1-(4-cyanophenyl)guanidine membrane absorbing liquid electrolyte as CGPEs, and it has a relatively high ionic conductivity of $2.32 \times 10^{-4} \, S \, cm^{-1}$. From their results, there are three reasons accounting for the high ionic conductivity. The first reason is the 3D porous structure of the PVDF-HFP provides continuous pathways for sodium ions. The second reason is that the addition of passive ceramic filler SnO_2 helps decrease the crystallinity of PVDF-HFP, which is benefit for the sodium ion migration. The last one is that introduction of 1-(4-cyanophenyl)guanidine forms a new pathway for sodium ion transportation because of strong interaction between sodium ions and imino nitrogen atoms.

The active filler $Na_2Zn_2TeO_6$ modified CGPE was reported in 2021.[118] The addition of $Na_2Zn_2TeO_6$ fillers leads to a decreased resistance, which is likely due to enhanced ionic conductivity (Figure 16a). The main reason for the improvement of the ionic conductivity of the CGPE is due mainly to the increase of liquid electrolyte uptake, decrease of crystallinity degree and improvement of porosity. The highest ionic conductivity at room temperature is obtained when the addition of $Na_2Zn_2TeO_6$ filler reaches 4 wt% (Figure 16b). Compared with non-filler-added electrolytes, the addition of $Na_2Zn_2TeO_6$ fillers improves the

ChemSusChem

Review
doi.org/10.1002/cssc.202202152

Chemistry
Europe
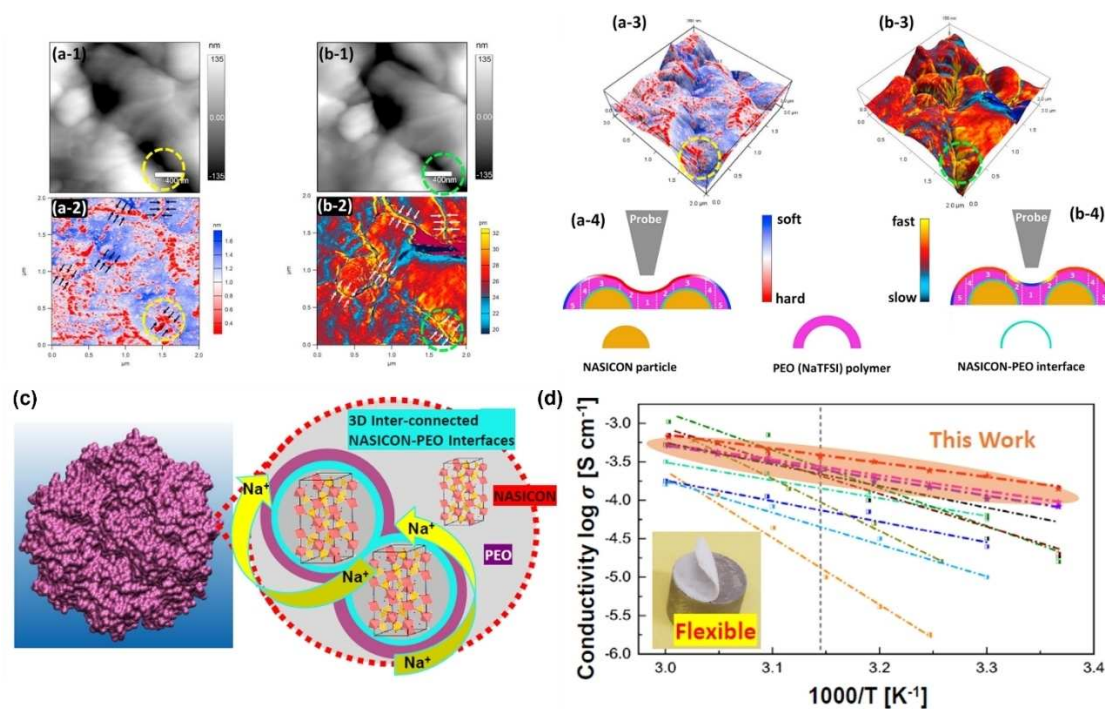European Chemical
Societies Publishing

Figure 14. Bimodal-AFM: (a-1) topography, (a-2) amplitude, (a-3) 3D topography profile overlapped with amplitude scale, and (a-4) schematic diagram (the outmost color strip represents the amplitude scale); ESM at the same position: (b-1) topography, (b-2) amplitude, (b-3) 3D topography profile overlapped with amplitude scale, and (b-4) schematic illustration (the outmost color strip represents the ESM amplitude scale). (c) Schematic illustration for the fabrication of NASICON/PEO composite electrolytes; (d) Comparison of the conductivities between the reported work and other reported counterparts for sodium batteries (dash line indicates 45 °C in temperature). Reproduced with permission.[112] Copyright 2020, Elsevier.
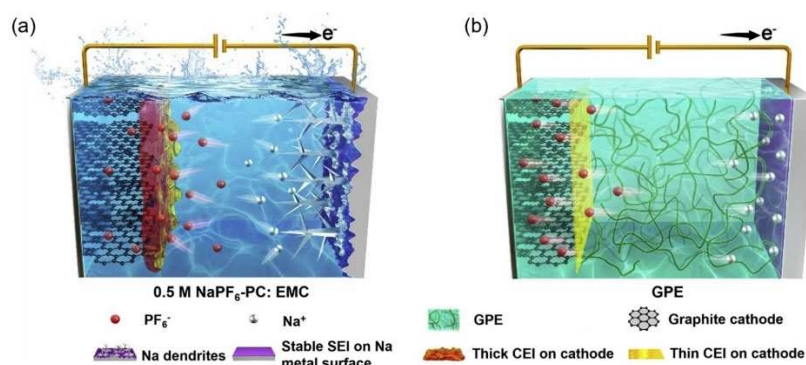

Figure 15. Schematic illustration of dual-ion sodium metal batteries using 0.5 M NaPF$_6$–PC:EMC liquid electrolyte (left) or GPE (right). Reproduced with permission.[117] Copyright 2020, Elsevier.

ionic conductivity under both low and high temperatures (Figure 16c). As a sodium conductor, the addition of Na$_2$Zn$_2$TeO$_6$ also provides a fast ion transport pathway at the interface of polymer and ceramic and thus leads to an enhanced ionic conductivity.

Mei et al.[119] also investigated the active filler Na$_3$Sc$_2$P$_3$O$_{12}$ of different crystal phases adding into CGPEs. The conclusions were basically the same. The addition of Na$_3$Sc$_2$P$_3$O$_{12}$ really increases the ionic conductivity. Despite the different crystal phases have slightly different ability on improving ionic conductivity, which is the γ phase performs better than the β and α phases, the conductive Na$_3$Sc$_2$P$_3$O$_{12}$ plays an important

role in the enhancement of CGPEs. Sodium ions can quickly transport at the interface between polymer and ceramic for the newly formed fast ion pathways. The decrease of crystallinity, improvement of liquid electrolyte absorption as well as the increased pores in the polymer matrix are all accounting for the enhancement of ionic conductivity.

Although the high ionic conductivities of the CGPEs are caused by the liquid components, the ceramic powders also help to decrease the crystallinity of polymer matrices and provide new sodium ion transport pathways. Compared with CPEs, the ceramic powders in CGPEs also exhibit the outstanding ability of increasing the liquid electrolyte uptake.[120]
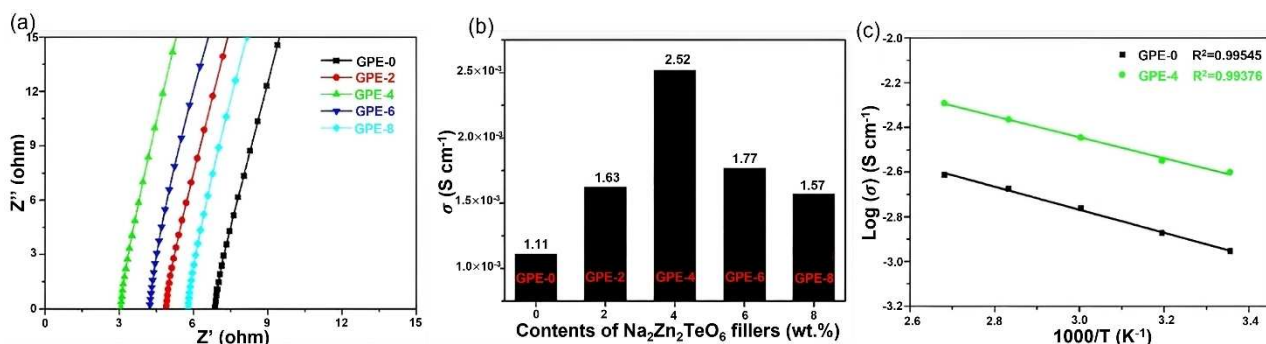
ChemSusChem

Review

doi.org/10.1002/cssc.202202152

Chemistry Europe
European Chemical
Societies Publishing

Figure 16. (a) Nyquist curves, (b) ionic conductivity at room temperature of the obtained GPEs membranes modified with variable $Na_2Zn_2TeO_6$ filler contents, and (c) the temperature dependence of ion conductivity. Reproduced with permission.[118] Copyright 2020, John Wiley and Sons.

The higher the ability of absorbing liquid electrolytes, the higher the ionic conductivities of CGPEs would be. Therefore, the ceramic powders in the CGPEs play a crucial role in both the enhancement of ionic conductivities and mechanical properties.

6. Perspectives

In the near future, sodium-ion batteries are promising candidates to replace lithium-ion batteries in the field of large-scale energy storage systems, because the cost of lithium-ion batteries is continuously rising due to the limited lithium resources. However, the energy density of sodium-ion batteries still cannot be comparable with that of lithium-ion batteries for portable devices, since they cannot satisfy both high energy capacity and light weight at the same time. Aside from the energy density, safety is another concern, particularly for vehicles. Therefore, solid-state electrolytes have been investigated with a view to replacing the liquid organic electrolytes to achieve high safety and high energy density. As the low room-temperature ionic conductivity of solid polymer electrolytes and the brittleness of inorganic solid electrolytes limit their practical application, CPEs have shown their promise, since they combine the advantages of high room-temperature ionic conductivity from the inorganic ion conductors with the high flexibility of polymers. Having said that, the ionic conductivities of the reported CPEs are still unable to satisfy the standards for practical application and, in addition, the issues associated with interfacial contacts are extremely important and should also be addressed as one of the key parameters. To address this, gel composite polymer electrolytes, which contain some liquid phases, are proposed and also demonstrate high ionic conductivity and particularly maintain a good electrode/electrolyte interface by liquid penetration. They can be considered as quasi solid-state, but still cannot completely eliminate the potential hazards. Therefore, design of CPEs with high ionic conductivity and at the same time with good wetting between the electrode and the electrolyte is the key to success of solid-state sodium ion batteries.

Conflict of Interest

The authors declare no conflict of interest.

[1] T. Chen, L. Qiu, Z. Yang, Z. Cai, J. Ren, H. Li, H. Lin, X. Sun, H. Peng, *Angew. Chem. Int. Ed.* **2012**, *51*, 11977.

[2] Z. Liang, C. Qu, W. Guo, R. Zou, Q. Xu, *Adv. Mater.* **2018**, *30*, 1702891.

[3] L. Dai, D. W. Chang, J. B. Baek, W. Lu, *Small* **2012**, *8*, 1130.

[4] A. A. Dar, J. Hameed, C. Huo, M. Sarfraz, G. Albasher, C. Wang, A. Nawaz, *Fuel* **2022**, *314*, 123094.

[5] A. G. Olabi, M. A. Abdelkareem, *Renewable Sustainable Energy Rev.* **2022**, *158*, 112111.

[6] J. Sun, J. A. Sam, O. Y. Wang, Z. Wang, K. Zeng, L. Lu, *Funct. Mater. Lett.* **2022**, *15*, 2251033.

[7] T. Guozden, J. P. Carbajal, E. Bianchi, A. Solarte, *Front. Energy Res.* **2020**, *8*, 16.

[8] Z. Yang, J. Zhang, M. C. Kintner-Meyer, X. Lu, D. Choi, J. P. Lemmon, J. Liu, *Chem. Rev.* **2011**, *111*, 3577.

[9] Y. Hu, W. Zha, Y. Li, X. Wu, Z. Wen, *Funct. Mater. Lett.* **2020**, *14*, 2141002.

[10] Y. Jiang, Y. Wang, J. Ni, L. Li, *InfoMat* **2021**, *3*, 339.

[11] H. Wang, J. Li, Y. Yin, L. Wang, P. Zhang, X. Lai, B. Yue, Y. Li, X. Hu, D. He, *Funct. Mater. Lett.* **2021**, *15*, 2250003.

[12] W. Hu, S. Wang, L. Peng, X. Hu, *Funct. Mater. Lett.* **2021**, *14*, 2143008.

[13] S. Zhang, J. Xie, P. Zhang, X. Zhao, *Funct. Mater. Lett.* **2021**, *14*, 2151033.

[14] Y. Wang, S. Song, C. Xu, N. Hu, J. Molenda, L. Lu, *Nano Mater. Sci.* **2019**, *1*, 91.

[15] X. Lu, C.-L. Tsai, S. Yu, H. He, O. Camara, H. Tempel, Z. Liu, A. Windmüller, E. V. Alekseev, S. Basak, L. Lu, R.-A. Eichel, H. Kungl, *Funct. Mater. Lett.* **2022**, *15*, 2240001.

[16] T. Zhao, S. Chen, X. Gao, Y. Zhang, *Funct. Mater. Lett.* **2021**, *14*, 2150029.

[17] D. B. Christoph Vaalma, M. Weil, S. Passerini, *Nat. Rev. Mater.* **2018**, *3*, 18013.

[18] L. Wang, Y. Wang, G. Jiang, J. Ni, L. Li, *Funct. Mater. Lett.* **2021**, *14*, 2143001.

[19] J. Zhang, H. Wen, L. Yue, J. Chai, J. Ma, P. Hu, G. Ding, Q. Wang, Z. Liu, G. Cui, L. Chen, *Small* **2017**, *13*, 1601530.

[20] J. Ni, L. Li, J. Lu, *ACS Energy Lett.* **2018**, *3*, 1137.

[21] B. Sun, J. Ni, *Funct. Mater. Lett.* **2022**, *15*, 2250019.

[22] P. Wang, H. Zhang, J. Chai, T. Liu, R. Hu, Z. Zhang, G. Li, G. Cui, *Solid State Ionics* **2019**, *337*, 140.

[23] J. Wei, Z. Yang, Z. Li, G. Lu, C. Xu, *Funct. Mater. Lett.* **2022**, *15*, 2250015.

[24] D. Ren, X. Feng, L. Liu, H. Hsu, L. Lu, L. Wang, X. He, M. Ouyang, *Energy Storage Mater.* **2021**, *34*, 563.

[25] Y. J. Park, M. K. Kim, H. S. Kim, B. M. Lee, *J. Toxicol. Environ. Health Part B* **2018**, *21*, 370.

[26] L. He, J. A. S. Oh, J. J. J. Chua, H. Zhou, *Funct. Mater. Lett.* **2020**, *14*, 2130002.

[27] J. Ni, L. Li, *Adv. Mater.* **2020**, *32*, 2000288.

[28] Q. Yu, Q. Lu, X. Qi, S. Zhao, Y.-B. He, L. Liu, J. Li, D. Zhou, Y.-S. Hu, Q.-H. Yang, F. Kang, B. Li, *Energy Storage Mater.* **2019**, *23*, 610.

[29] H. Nagai, S. Song, *Funct. Mater. Lett.* **2021**, *14*, 2102001.

[30] Y. Lu, L. Li, Q. Zhang, Z. Niu, J. Chen, *Joule* **2018**, *2*, 1747.

[31] J. A. S. Oh, L. He, B. Chua, K. Zeng, L. Lu, *Energy Storage Mater.* **2021**, *34*, 28.

[32] L. He, J. A. S. Oh, J. J. J. Chua, H. Zhou, *Funct. Mater. Lett.* **2020**, *14*, 2130001.

[33] Y. Zhang, Z. Zheng, X. Liu, M. Chi, Y. Wang, *J. Electrochem. Soc.* **2019**, *166*, A515.

[34] C. Zhao, L. Liu, X. Qi, Y. Lu, F. Wu, J. Zhao, Y. Yu, Y.-S. Hu, L. Chen, *Adv. Energy Mater.* **2018**, *8*, 1703012.

[35] J. Gao, J. Wu, S. Han, J. Zhang, L. Zhu, Y. Wu, J. Zhao, W. Tang, *Funct. Mater. Lett.* **2021**, *14*, 2140001.

[36] Q. Zhao, S. Stalin, C.-Z. Zhao, L. A. Archer, *Nat. Rev. Mater.* **2020**, *5*, 229.

[37] J. Gan, Y. Huang, Z. Guo, S. Li, W. Ren, X. Li, M. Wang, Y. Lin, L. Liu, *Funct. Mater. Lett.* **2021**, *14*, 2151017.

[38] L. Han, J. Wang, X. Mu, T. Wu, C. Liao, N. Wu, W. Xing, L. Song, Y. Kan, Y. Hu, *J. Colloid Interface Sci.* **2021**, *585*, 596.

[39] W. Liu, D. Lin, J. Sun, G. Zhou, Y. Cui, *ACS Nano* **2016**, *10*, 11407.

[40] S. Tamainato, D. Mori, Y. Takeda, O. Yamamoto, N. Imanishi, *ChemistrySelect* **2022**, *7*, e202201667.

[41] S. Liu, W. Liu, D. Ba, Y. Zhao, Y. Ye, Y. Li, J. Liu, *Adv. Mater.* **2022**, e2110423.

[42] P. Yao, H. Yu, Z. Ding, Y. Liu, J. Lu, M. Lavorgna, J. Wu, X. Liu, *Front. Chem.* **2019**, *7*, 522.

[43] X. Yu, A. Manthiram, *Energy Storage Mater.* **2021**, *34*, 282.

[44] S. Tang, W. Guo, Y. Fu, *Adv. Energy Mater.* **2020**, *11*, 2000802.

[45] D. K. Maurya, R. Dhanusuraman, Z. Guo, S. Angaiah, *Adv. Compos. Hybrid Mater.* **2022**, *5*, 2651.

[46] F. Gebert, J. Knott, R. Gorkin, S.-L. Chou, S.-X. Dou, *Energy Storage Mater.* **2021**, *36*, 10.

[47] S. Xia, X. Wu, Z. Zhang, Y. Cui, W. Liu, *Chem* **2019**, *5*, 753.

[48] V. Bocharova, A. P. Sokolov, *Macromolecules* **2020**, *53*, 4141.

[49] Q. Yang, A. Wang, J. Luo, W. Tang, *Chin. J. Chem. Eng.* **2022**, *43*, 202.

[50] R. Dupon, B. Papke, M. Ratner, D. Whitmore, D. Shriver, *J. Am. Chem. Soc.* **1982**, *104*, 6247.

[51] B. Papke, M. Ratner, D. Shriver, *J. Phys. Chem. Solids* **1981**, *42*, 493.

[52] B. Papke, M. Ratner, D. Shriver, *J. Electrochem. Soc.* **1982**, *129*, 1694.

[53] J. Parker, P. Wright, C. Lee, *Polymer* **1981**, *22*, 1305.

[54] X. Qi, Q. Ma, L. Liu, Y.-S. Hu, H. Li, Z. Zhou, X. Huang, L. Chen, *ChemElectroChem* **2016**, *3*, 1741.

[55] A. Boschin, P. Johansson, *Electrochim. Acta* **2015**, *175*, 124.

[56] M. Patel, K. G. Chandrappa, A. J. Bhattacharyya, *Solid State Ionics* **2010**, *181*, 844.

[57] P. B. Bhargav, V. Mohan, A. Sharma, V. Rao, *J. Appl. Polym. Sci.* **2008**, *108*, 510.

[58] P. B. Bhargav, V. M. Mohan, A. Sharma, V. N. Rao, *Int. J. Polym. Mater.* **2007**, *56*, 579.

[59] R. Sathiyamoorthi, R. Chandrasekaran, S. Selladurai, T. Vasudevan, *Ionics* **2003**, *9*, 404.

[60] K. N. Kumar, T. Sreekanth, M. J. Reddy, U. S. Rao, *J. Power Sources* **2001**, *101*, 130.

[61] M. Vahini, M. Muthuvinayagam, *Mater. Lett.* **2019**, *238*, 17.

[62] G. S. Sundari, K. V. Kumar, N. K. Jyothi, P. A. Reddy, *Asian J. Chem.* **2013**, *25*, S459.

[63] J. W. Fergus, *Solid State Ionics* **2012**, *227*, 102.

[64] D. E. Fenton, J. M. Parker, P. V. Wright, *Polymer* **1973**, *14*, 589.

[65] K. West, B. Zachau-Christiansen, T. Jacobsen, E. Hiort-Lorenzen, S. Skaarup, *Br. Polym. J.* **1988**, *20*, 243.

[66] Y. Ma, M. Doyle, T. F. Fuller, M. M. Doeff, L. C. De Jonghe, J. Newman, *J. Electrochem. Soc.* **1995**, *142*, 1859.

[67] A. \Ferry, M. M. Doeff, L. C. De Jonghe, *J. Electrochem. Soc.* **1998**, *145*, 1586.

[68] Z. Zou, Y. Li, Z. Lu, D. Wang, Y. Cui, B. Guo, Y. Li, X. Liang, J. Feng, H. Li, C. W. Nan, M. Armand, L. Chen, K. Xu, S. Shi, *Chem. Rev.* **2020**, *120*, 4169.

[69] T. Famprikis, P. Canepa, J. A. Dawson, M. S. Islam, C. Masquelier, *Nat. Mater.* **2019**, *18*, 1278.

[70] X. Feng, H. Fang, N. Wu, P. Liu, P. Jena, J. Nanda, D. Mitlin, *Joule* **2022**, *6*, 543.

[71] J. F. Wu, R. Zhang, Q. F. Fu, J. S. Zhang, X. Y. Zhou, P. Gao, C. H. Xu, J. Liu, X. Guo, *Adv. Funct. Mater.* **2020**, *31*, 2008165.

[72] Y.-F. Y. Yao, J. Kummer, *J. Inorg. Nucl. Chem.* **1967**, *29*, 2453.

[73] C. Zhu, J. Xue, *J. Alloys Compd.* **2012**, *517*, 182.

[74] W. Archer, R. Armstrong, D. Sellick, W. Bugden, J. Duncan, *J. Mater. Sci.* **1980**, *15*, 2066.

[75] J. Dygas, G. Fafilek, M. Breiter, *Solid State Ionics* **1999**, *119*, 115.

[76] G. Chen, J. Lu, X. Zhou, L. Chen, X. Jiang, *Ceram. Int.* **2016**, *42*, 16055.

[77] G. May, A. Hooper, *J. Mater. Sci.* **1978**, *13*, 1480.

[78] A. Hooper, *J. Phys. D* **1977**, *10*, 1487.

[79] C. Zhu, Y. Hong, P. Huang, *J. Alloys Compd.* **2016**, *688*, 746.

[80] Y. Sheng, P. Sarkar, P. S. Nicholson, *J. Mater. Sci.* **1988**, *23*, 958.

[81] X. Lu, M. E. Bowden, V. L. Sprenkle, J. Liu, *Adv. Mater.* **2015**, *27*, 5915.

[82] G. Chen, J. Lu, L. Li, L. Chen, X. Jiang, *J. Alloys Compd.* **2016**, *673*, 295.

[83] Q. Ma, F. Tietz, *ChemElectroChem* **2020**, *7*, 2693.

[84] Q. Huang, G. Chen, P. Zheng, W. Li, T. Wu, *Funct. Mater. Lett.* **2021**, *14*, 2310005.

[85] J. B. Goodenough, H.-P. Hong, J. Kafalas, *Mater. Res. Bull.* **1976**, *11*, 203.

[86] H. Park, K. Jung, M. Nezafati, C. S. Kim, B. Kang, *ACS Appl. Mater. Interfaces* **2016**, *8*, 27814.

[87] M. Samiee, B. Radhakrishnan, Z. Rice, Z. Deng, Y. S. Meng, S. P. Ong, J. Luo, *J. Power Sources* **2017**, *347*, 229.

[88] Z. Zhang, Q. Zhang, J. Shi, Y. S. Chu, X. Yu, K. Xu, M. Ge, H. Yan, W. Li, L. Gu, *Adv. Energy Mater.* **2017**, *7*, 1601196.

[89] Q. Ma, M. Guin, S. Naqash, C.-L. Tsai, F. Tietz, O. Guillon, *Chem. Mater.* **2016**, *28*, 4821.

[90] M. Guin, F. Tietz, O. Guillon, *Solid State Ionics* **2016**, *293*, 18.

[91] M. Guin, F. Tietz, *J. Power Sources* **2015**, *273*, 1056.

[92] M. Jansen, U. Henseler, *J. Solid State Chem.* **1992**, *99*, 110.

[93] A. Hayashi, K. Noi, A. Sakuda, M. Tatsumisago, *Nat. Commun.* **2012**, *3*, 856.

[94] V. S. Kandagal, M. D. Bharadwaj, U. V. Waghmare, *J. Mater. Chem. A* **2015**, *3*, 12992.

[95] H.-L. Yang, B.-W. Zhang, K. Konstantinov, Y.-X. Wang, H.-K. Liu, S.-X. Dou, *Adv. Energy Sustain. Res.* **2021**, *2*, 2000057.

[96] W. D. Richards, T. Tsujimura, L. J. Miara, Y. Wang, J. C. Kim, S. P. Ong, I. Uechi, N. Suzuki, G. Ceder, *Nat. Commun.* **2016**, *7*, 11009.

[97] Y. Wang, W. D. Richards, S.-H. Bo, L. J. Miara, G. Ceder, *Chem. Mater.* **2017**, *29*, 7475.

[98] J. W. Heo, A. Banerjee, K. H. Park, Y. S. Jung, S.-T. Hong, *Adv. Energy Mater.* **2018**, *8*, 1702716.

[99] L. Long, S. Wang, M. Xiao, Y. Meng, *J. Mater. Chem. A* **2016**, *4*, 10038.

[100] F. Croce, L. Persi, B. Scrosati, F. Serraino-Fiory, E. Plichta, M. Hendrickson, *Electrochim. Acta* **2001**, *46*, 2457.

[101] P. M. Veelken, M. Wirtz, R. Schierholz, H. Tempel, H. Kungl, R.-A. Eichel, F. Hausen, *Nanomaterials* **2022**, *12*, 654.

[102] A. Dey, T. Ghoshal, S. Karan, S. De, *J. Appl. Phys.* **2011**, *110*, 043707.

[103] A. Chandra, A. Chandra, K. Thakur, *Arab. J. Chem.* **2016**, *9*, 400.

[104] A. Chandra, A. Chandra, R. Dhundhel, A. Jain, A. Bhatt, *Russ. J. Electrochem.* **2021**, *57*, 375.

[105] A. Dey, T. Ghoshal, S. Karan, S. K. De, *J. Appl. Phys.* **2011**, *110*, 043707.

[106] L. Xu, J. Li, W. Deng, L. Li, G. Zou, H. Hou, L. Huang, X. Ji, *Mater. Chem. Front.* **2021**, *5*, 1315.

[107] J. Serra Moreno, M. Armand, M. B. Berman, S. G. Greenbaum, B. Scrosati, S. Panero, *J. Power Sources* **2014**, *248*, 695.

[108] Y. Yao, Z. Liu, X. Wang, J. Chen, X. Wang, D. Wang, Z. Mao, *J. Mater. Sci.* **2021**, *56*, 9951.

[109] Z. Zhang, X. Xu, X. Rong, Y.-S. Hu, H. Li, X. Huang, L. Chen, *J. Power Sources* **2017**, *372*, 270.

[110] X. Yu, L. Xue, J. B. Goodenough, A. Manthiram, *ACS Materials Lett.* **2019**, *1*, 132.

[111] Y. Lu, L. Li, Q. Zhang, Y. Cai, Y. Ni, J. Chen, *Chem. Sci.* **2022**, *13*, 3416.

ChemSusChem

Review
doi.org/10.1002/cssc.202202152

Chemistry Europe
European Chemical
Societies Publishing

[112] Y. Wang, Z. Wang, J. Sun, F. Zheng, M. Kotobuki, T. Wu, K. Zeng, L. Lu, *J. Power Sources* **2020**, *454*, 227949.

[113] V. P. Hoang Huy, S. So, J. Hur, *Nanomaterials* **2021**, *11*, 614.

[114] X. Xu, J. Gan, Y. Huang, J. Liu, L. Zhao, C. Li, J. Chen, X. Li, M. Wang, Y. Lin, *Funct. Mater. Lett.* **2021**, *15*, 2251010.

[115] S. A. Hashmi, M. Y. Bhat, M. K. Singh, N. T. K. Sundaram, B. P. C. Raghupathy, H. Tanaka, *J. Solid State Electrochem.* **2016**, *20*, 2817.

[116] Y. Zhao, H. Liu, X. Meng, A. Liu, Y. Chen, T. Ma, *Chem. Eng. J.* **2022**, *431*, 133922.

[117] X. Xu, K. Lin, D. Zhou, Q. Liu, X. Qin, S. Wang, S. He, F. Kang, B. Li, G. Wang, *Chem* **2020**, *6*, 902.

[118] X. Wang, Z. Liu, Y. Wang, J. Chen, Z. Mao, D. Wang, *ChemElectroChem* **2020**, *7*, 5021.

[119] W. Mei, X. Wang, Y. Wang, J. Chen, Z. Mao, D. Wang, *J. Solid State Chem.* **2021**, *302*, 122459.

[120] M. Walkowiak, M. Osińska, T. Jesionowski, K. Siwińska-Stefańska, *Open Chemistry* **2010**, *8*, 1311.

REVIEW

Best of both worlds: Solid-state inorganic and polymer electrolytes for sodium-ion batteries are safer than commercial liquid organic electrolytes but suffer from rigidity and low room-temperature ionic conductivities, respectively. This Review focuses on composite polymer electrolytes made up of inorganic solid electrolytes and solid polymer electrolytes, which can realize both high ionic conductivity and flexibility.
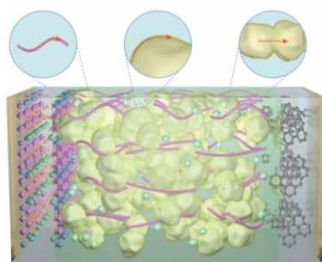
X. Xu, Dr. Y. Wang*, Q. Yi, X. Wang, Dr. R. A. Paredes Camacho, Prof. H. Kungl, Prof. R. Eichel, Prof. L. Lu*, Prof. H. Zhang*

1 – 19

Ion Conduction in Composite Polymer Electrolytes: Potential Electrolytes for Sodium-Ion Batteries